A STUDY OF COSMIC RAY VARIABILITY DURING A SOLAR MAGNETIC CYCLE (SOLAR CYCLES 23 AND 24)

ABSTRACT

We investigated variations in Cosmic Ray (CR) intensities during Solar Cycles (SC) 23 and 24. Using data from the Mexico neutron monitor, solar wind parameters (speed, temperature, plasma density), geomagnetic indices (Kp, Dst, ap) from OMNI, and sunspot numbers from SISLO, we analyzed CR intensities during the ascending (ASC) and declining (DSC) phases of each cycle. Our analysis, using distribution plots and regression methods, showed higher CR intensities during the DSC phases compared to the ASC phases for both cycles. Additionally, average CR values were higher during SC 24 than SC 23. These variations are linked to differences in sunspot numbers, solar wind parameters, and geomagnetic indices, differences in magnetic transport across the Sun differ between the ASC and DSC phases, with SC 24 exhibiting weaker meridional flow compared to SC 23. In summary, we find that for the complete Hale cycle we describe, the CR intensities are modulated to different extents during different solar cycle phases and that the modulation varies from one solar cycle to another.

Keywords: Cosmic Rays, Method: Data Analysis, Method: Statistical, Sunspot Number

1 INTRODUCTION

Cosmic rays (CRs) are high-energy particles, primarily protons and atomic nuclei, that travel through space at nearly the speed of light. They originate from various sources, including the Sun, distant supernovae, and other energetic astrophysical phenomena. These particles can be detected on Earth or in space via their interactions with the atmosphere or detectors, where they create showers of secondary particles. Cosmic rays are classified based on their energy levels, ranging from a few MeV to more than 10 eV (Rees & Sargent, 1968; Zweibel, 2013; Sparvoli & Martucci, 2022). Most CRs are protons, but can also include heavier nuclei and electrons. Research suggests that they consist of 98% atomic nuclei and 2% electrons, with the nuclei including roughly 87% protons, 12% helium, and 1% heavier elements (Simpson 1983). Their study provides insights into high-energy processes in the universe, and their interactions help us understand astrophysical environments like the interstellar medium.

When CRs enter the Earth's atmosphere, they collide with atmospheric molecules, creating secondary particles in a phenomenon known as an air shower (Auger et al., 1939; Rossi, 1930). CRs are classified into two main types based on their origin: Galactic CRs, which originate from sources within our galaxy, such as supernovae and other stellar events (Vaclav, 2009; Ackermann et al., 2013), and extragalactic CRs (Sharma, 2008; Abramowski et al., 2016), which are believed to come from outside our galaxy, likely from extremely energetic events like active galactic nuclei, gamma-ray bursts, and magnetars (Vannoni et al., 2011; Hjorth & Bloom, 2012). The energy density of CRs averages around $1 eV/cm^3$ of interstellar space

CRs can also be categorized by their energy levels; for example, low-energy CRs are trapped by the Earth's magnetic field and interact with the upper atmosphere, while high-energy CRs penetrate deeper into the atmosphere and are detectable by ground-based instruments

(Anchordoqui et al., 2003; Abe et al., 2016). Studying cosmic rays allows scientists to gain insights into fundamental processes in the universe, such as the behavior of high-energy particles and the conditions in distant astrophysical objects.

Sunspots are large solar storms that are difficult to predict (Echer et al., 2004; Kane, 2006). They appear as dark areas on the surface of the Sun due to intense magnetic activity, inhibiting convection and leading to lower surface temperatures than the surrounding areas. Their formation is linked to the Sun's magnetic field, as magnetic flux tubes rise through the solar surface due to buoyancy, creating localized areas of strong magnetic fields that become sunspots. These spots are important indicators of solar magnetic activity, which fluctuates over an approximately 11-year solar cycle (Solanki, 2003; Balogh, et al., 2014). Sunspots have effects beyond the Sun itself. They influence solar radiation and can impact space weather, including solar flares and coronal mass ejections. These solar phenomena can affect satellite communications, GPS systems, and power grids on Earth (Ruzmaikin, 2001; Solanki, 2002).

The number, coverage area, and intensity of sunspots vary in a cyclic pattern with a period of approximately 11 years, known as the solar cycle (SC). This cycle is monitored by counting sunspots, the most easily observed features of solar activity, and has been tracked since the early 1600s (Hoyt & Schatten, 1979, 1998; Kane, 2006). Sunspots can appear as single, isolated dark central regions called umbrae surrounded by a less dark pattern called penumbra, or in groups (Spiegel, 1994). At the core of the approximately 11-year cycle is the oscillating magnetic dynamo within the Sun, which changes approximately every 22 years (Denkmayr and Cugnon, 1997; Zhan et al., 2004; Xu et al., 2008). Sunspot cycles vary in size and length, making it challenging to describe their shape with a universal function (Layden et al., 1991; Conway, 1998). Many authors have attempted to describe these cycles as periodic phenomena, leading to a wealth of literature on the subject (Denkmayr and Cugnon, 1997; Hanslmeier et al., 1999; Zhan et al., 2004; Xu et al., 2008).

Numerous studies have examined the correlation between solar activities and the impact on CR intensity. Although CR intensity remains relatively steady outside the heliosphere, it varies during its journey through the heliosphere due to solar activities and changes in the interplanetary magnetic fields (Agrawal et al., 1993; Mavromichalaki et al., 1998; Bhattacharya and Roy, 2014). The fluctuations in CR intensities are mainly attributed to the outward release of solar outputs such as solar wind, coronal mass ejections (CME), and solar flares. The solar wind influences the propagation of CRs, altering their paths and energies. In addition, changes in the configuration and strength of the heliospheric magnetic field can significantly modify CRs.

The Sun goes through a cycle called the Solar Cycle (SC) during which its magnetic field changes polarity. This cycle affects the level of solar modulation of CRs. The Sun's magnetic field drives activities such as sunspots, flares, prominence eruptions, and Coronal Mass Ejections (CMEs), which in turn influence Earth's upper atmosphere, magnetosphere, ionosphere, and near-Earth space environment. These solar disturbances also lead to fluctuations in CR flux, causing sudden increases known as Ground-Level Enhancements (GLEs) and depressions called Forbush Decreases (FD). These variations show periodic changes including daily anisotropies, an 11-year solar cycle, 27-day Sun-rotation short-term variations, and rapid irregular changes

(Forbush, 1946; Simpson, 1990; Jothe et al. 2010; Shrivastava et al. 2011; Gopalswamy et al., 2014; Okike et al. 2021; Okike and Alhassan 2021; Singh et al., 2023).

Over the years, several researchers (Cliver and Ling, 2001; Van Allen, 2000; Persai et al., 2015; Chaurasiya et al., 2023) have discovered a strong correlation between sunspot numbers (SSN) and various phenomena such as the modulation of CR intensity, and CME (Onuchukwu, 2018). Therefore, it has been suggested that SSN could act as a proxy for long-term changes in the interplanetary magnetic field (IMF) over extended periods, consequently impacting CR intensity. According to Usoskin et al., (2005), the long-term variation in CR intensity demonstrates a significant sensitivity to SSN during periods of low solar activity and relative invariance during times of higher solar activity.

This study seeks to investigate the fluctuation of CR intensity throughout the ascending (ASC) and declining (DSC) phases of SCs. CRs, composed of high-energy particles originating from sources beyond the solar system, exhibit varying levels of intensity influenced by the solar magnetic activity. During the ASC phase of solar cycles, solar magnetic activity gradually increases, reaching its peak at solar maximum, whereas during the DSC phase, solar activity diminishes towards solar minimum. The central questions guiding this research are outlined as follows:

- What is the temporal evolution of CR intensity during the ASC and DSC phases of SCs?
- Are there any correlations between CR intensity variations and solar activity such as SSN, and solar-terrestrial parameters (e.g. Solar Wind Speed (SWS), Solar Wind Temperature (SWT), Solar Wind Plasma Density (SWPD), Interplanetary Magnetic Field (IMF), geomagnetic activity indices like Dst, Kp and ap)?
- Are there potential differences in CR modulation mechanisms between the ASC and DSC phases of SCs?
- Identify any trends, periodicities, or anomalies in the CR intensity variations over solar magnetic cycles.

By addressing these issues, this study will help advance our understanding of the complex interplay between solar activity and CR modulation, shedding light on the underlying mechanisms driving CR variations throughout different phases of SCs. Furthermore, the findings will contribute to enhancing space weather forecasting capabilities and mitigating potential risks associated with cosmic ray exposure in various domains.

2 **Data: Data Description**

The daily average sunspot data were obtained from the World Data Center SILSO, Royal Observatory of Belgium, Brussels (http://www.sidc.be/SILSO/). According to SILSO, SC 23 started in August 1996, lasted for 12.25 years reached its maximum in November 2001, and ended in November 2008. SC 24, stated in December 2008, reached its maximum in April 2014, lasting for 11 years, and ending in November 2019.

The CR data utilized in this study were sourced from the neutron monitor located at the central campus of the National Autonomous University of Mexico (UNAM), accessible through http://www.cosmicrays.unam.mx/. Managed by the Cosmic Ray Group of the Geophysical Institute at UNAM, Mexico City, the detector has operated since January 1, 1990. Positioned at

19.33 deg N latitude, 260.83 deg E longitude, and an altitude of 2274 m, with an effective cutoff rigidity of 8.2 GV, it serves as a reliable source for CR measurements. Fig 6 of Okike et al., (2020) illustrates that comparable data can be retrieved from the High-Resolution Neutron Monitor Database (NMDB) at http://www.nmdb.eu, as also noted by Mavromichalaki et al., (2011). Our study focused on daily pressure-corrected CR data spanning from 1996 to 2019, encompassing SCs 23 and 24. Utilizing averaged CR data offers advantages, notably in mitigating the effects of CR diurnal anisotropy, as discussed by Dumbovic et al., (2011) and Belov et al., (2018).

The studies by Gopalswamy et al. (2014), Lingri et al. (2016), and Okike & Umahi (2019), etc. have identified SC 23 as a significant period of heightened solar activity. Additionally, SC 23, known for its prolonged duration and intense solar activity, was followed by SC 24, which was characterized by a delayed and subdued maximum. Therefore, studying CR variations during these highly active and subdued activity solar cycles, SCs 23 and 24, provides us with a valuable opportunity.

The daily average solar wind parameters between 1996 and 2019 (like IMF (nT)), SWT (K), SWPD (N/cm^3), SWS (km/s), and the geomagnetic activity indices - (Kp) (measured 3 hourly), Dst (measured 1 hourly), ap (measured 3 hourly)), were obtained from https://omniweb.gsfc.nasa.gov/.

We formed two subsamples for each SC: the ascending (ASC) phase and the declining (DSC) phase. According to SILSO, the ASC phase of SC 23 lasted from August 1996 to November 2001, while the DSC phase for SC 23 was from December 2011 to November 2012. For SC 24, the ASC phase was from December 2008 to April 2014, and the DSC phase was from May 2014 to November 2019.

3 Method of Analysis

We analyze the data by plotting the distribution (while checking for skewness, and kurtosis), plot the time series graph, and perform simple linear regression analysis to check for possible correlation between the parameters. The distribution of a data set in an analysis is essential for several reasons, which include:

i. Visualizing the distribution helps in understanding the underlying structure of the data. It allows analysts to see patterns, trends, and anomalies that might not be evident from raw numbers, especially, when comparing multiple data sets, distribution plots help in visually assessing similarities and differences in their shapes, centers, spreads, and tails.
ii. The distribution plots can reveal whether the data is normally distributed, skewed, or has other characteristics like bi-modality. This is important for choosing the right statistical methods and models.
iii. Distribution plots, such as histograms make it easier to spot outliers or unusual observations that could affect the analysis.
iv. Many statistical tests and models assume a specific distribution of the data (e.g., normality). Plotting the data helps in verifying these assumptions and deciding whether data transformations are needed.

v. Distribution plots are effective tools for communicating findings to a broader audience, including those who may not have a deep statistical background. They make complex data more accessible and interpretable.

Skewness measures the degree of asymmetry in a distribution. A positively skewed distribution exhibits numerous outliers in its right tail, whereas a negatively skewed distribution shows many outliers in its left tail. In a positively skewed distribution, the mean surpasses the median, whereas in a negatively skewed distribution, the median exceeds the mean. For large samples, the sample skewness is given as Cramer, 1997)

$$S_x = \frac{1}{n}\frac{\sum_{i=1}^{n}(\hat{X}-\langle X\rangle)^3}{\sigma^3} \quad (1)$$

where $\hat{X}$ is the mean, $\langle X\rangle$ is the median, σ is standard deviation, and n is the number of observations, a skewness value over 0.5 indicates a significant value of skewness.

Kurtosis (K) is the degree to which a distribution is more or less peaked in normal distribution. Kurtosis measures the peakedness or flatness of a distribution. A kurtosis value of 3 indicates a normal distribution (mesokurtic). If the kurtosis is greater than 3 (positive kurtosis), the distribution is more peaked (leptokurtic) than a normal distribution, with heavier tails. The sample kurtosis is given as (Cramer, 1997)

$$K = \frac{1}{n}\frac{\sum_{i=1}^{n}(\hat{X}-\langle X\rangle)^3}{\sigma^3} \quad (2)$$

Time series analysis is a specific way of analyzing a sequence of data points collected over an interval of time. In time series analysis, the analysts record data points at consistent intervals over a set period rather than just recording the data points intermittently or randomly. Time series analysis typically requires a large number of data points to ensure consistency and reliability. Correlation quantifies the extent of a linear relationship between two or more variables, indicating how changes in one variable are related to changes in another. The correlation coefficient, denoted as r, represents the strength of this linear relationship between two variables, X and Y, and it is given as (e.g. Fisher, 1915)

$$r = \frac{\sum_{i=1}^{n}(X_i-\bar{X})(Y_i-\bar{Y})}{\sqrt{\sum_{i=1}^{n}(X_i-\bar{X})^2(Y_i-\bar{Y})^2}} \quad (3)$$

where n is the number of each variable which must be equal, $\bar{X}$ and $\bar{Y}$ are the mean value of the variable X and Y respectively.

4 Results and Discussion

4.1 Time Series - Daily Variations

Figures 1-2 show the average daily variations of CR and SSN for the ASC and DSC phases of SC 23 and 24. The plot reveals higher CR intensity at the beginning and end of each SC, the CR intensity showed an inverse correlation with the SSN, with an overall higher CR intensity during SC 24 compared to SC 23 (Usoskin et al., 2002). The plots of the variation of daily average values of CR and SSN (see Figures 1-2) did not reveal clear trends due to rapid fluctuations. Therefore, we opted to plot the time series of variations of the monthly average values.

Plotting monthly averages instead of daily or yearly averages offers several key advantages in data analysis and visualization. Firstly, monthly averaging effectively smooths out daily fluctuations and random noise, which may obscure significant trends when working with daily data. This reduction in data volatility allows for a clearer view of the underlying patterns, as

noted in several studies on data smoothing techniques (Kass et al., 2018). Secondly, using monthly data facilitates the identification.

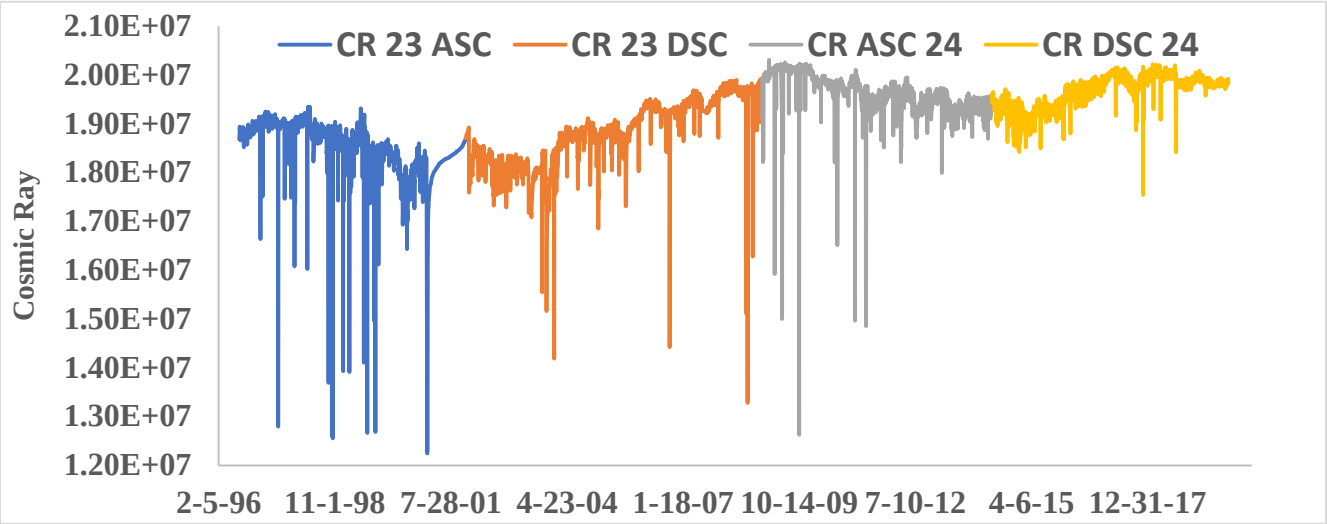

Fig. 1 Plot of Daily Variation of CR

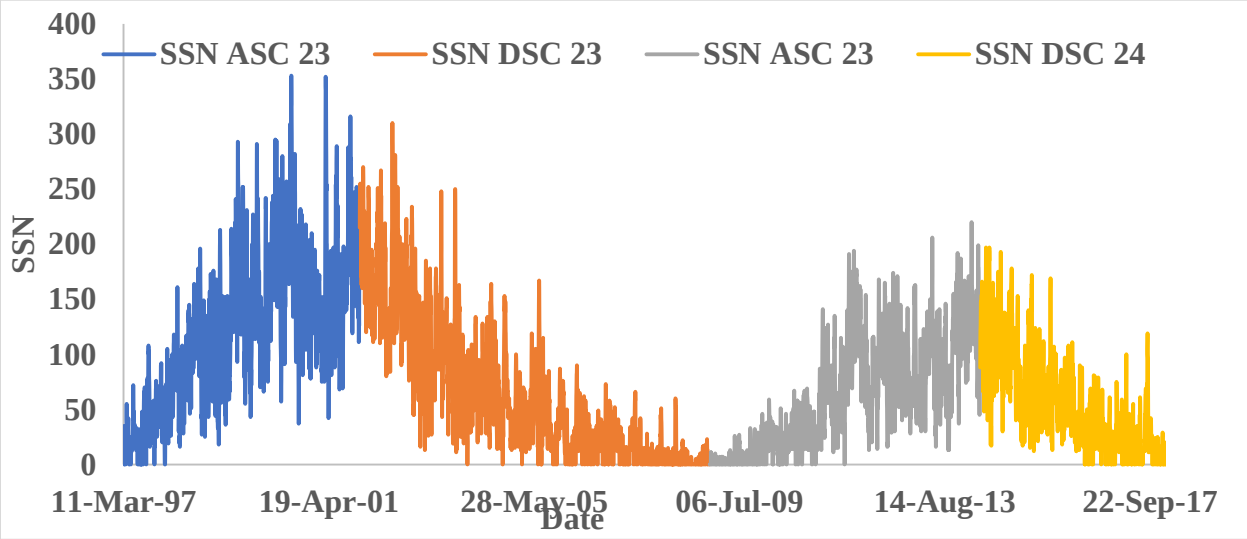

Fig. 2 Plot of Daily Variation of SSN

4.2 Monthly Average Time Series Plot

Figures 4-11 display the time series plots of monthly average values for the ASC and DSC phases of SCs 23 and 24. These plots include the monthly average of the CR intensity, the monthly average of the SSN, the monthly average of the solar-terrestrial parameters (IMF, SWS, SWT, and SWPD), and the monthly average of the geomagnetic activity indices (Kp, Dst, ap) for ASC and the DSC phases of SCs 23 and 24.

4.2.1. The Monthly Average Cosmic Ray, Sunspot Number, and IMF Variation for SCs 23 and 24

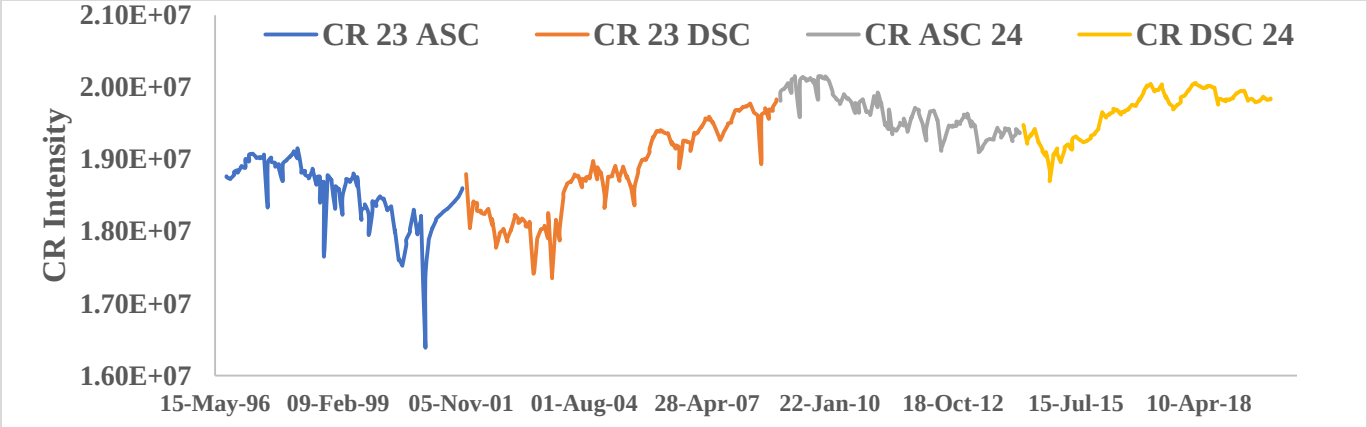

Fig. 3 Time Series Plot of the Monthly Average Values of CR Intensity Variation for the ASC and DSC Phases of SCs 23 and 24

Fig. 4 Time Series Plot of the Monthly Average Values of SSN Variation for the ASC and DSC Phases of SCs 23 and 24

Fig 3 plots the monthly average values for CR intensities for the ASC and DSC Phases of SCs 23 and 24. In SC 23, the intensity of CR was higher during the DSC phase (lowest monthly average values of (1.7×10^7 were recorded in July and November 2003) compared to the ASC phase with the lowest monthly average values recorded in October 1998 (1.8×10^7), July 2000 (1.8×10^7), and January 2001 (1.6×10^7). Similarly, in SC 24, CR intensity was higher during the DSC phase than the ASC phase. Overall, CR intensity was higher in SC 24 than in SC 23. The monthly average SSN values were higher in SC 23 than in SC 24.

Fig 4 plots the monthly average values for SSN for the ASC and DSC Phases of SCs 23 and 24. Generally, SSN values were higher during the ASC phases than the DSC phases for both cycles,

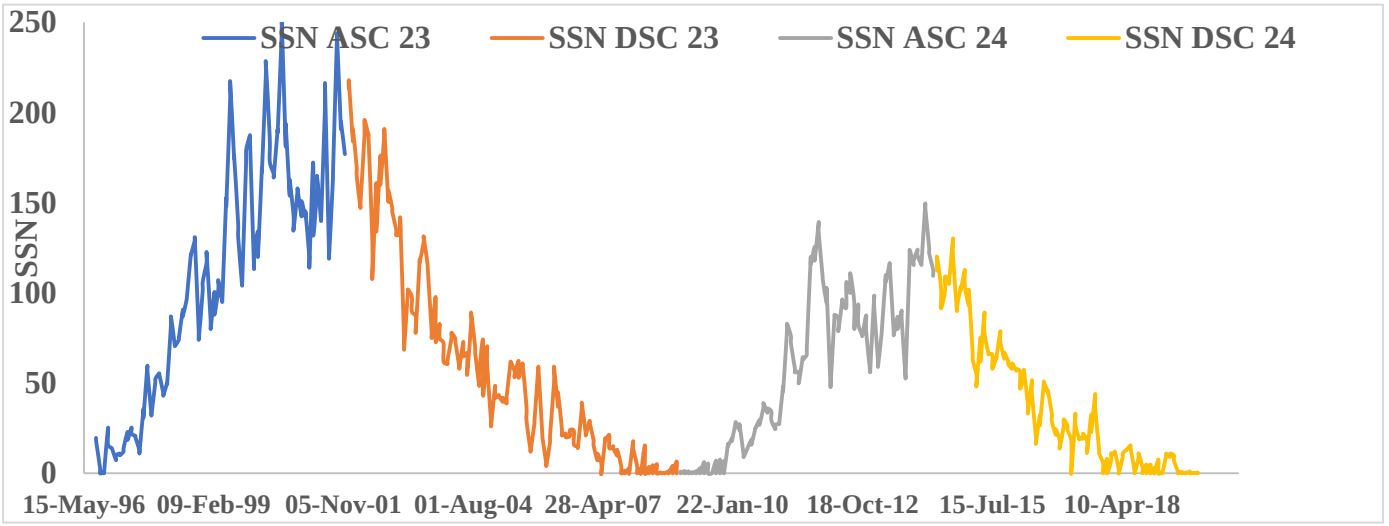

although the DSC phases lasted longer than the ASC phases in both solar cycles. The double hump (peak-dip-peak) that characterizes a SC (Ramesh, 2010, Onuchukwu 2018), occurred during the ASC phases of both SC. It is worth noting that CR values showed an inverse

relationship with SSN values in each phase of SC 23 and 24. This finding is consistent with the results reported by various authors e.g. Mishra (2005), Mishra & Mishra (2016), and Chaurasiya et al. (2023), etc.

Fig 5 is the plot of the monthly average values for the ASC and DSC Phases of SCs 23 and 24 for the IMF. The IMF displayed higher average monthly values in SC 23 than in SC 24. During SC 23, these IMF values were higher during the ASC phase than the DSC phase, whereas during SC 24, they were higher during the DSC phase than the ASC phase.

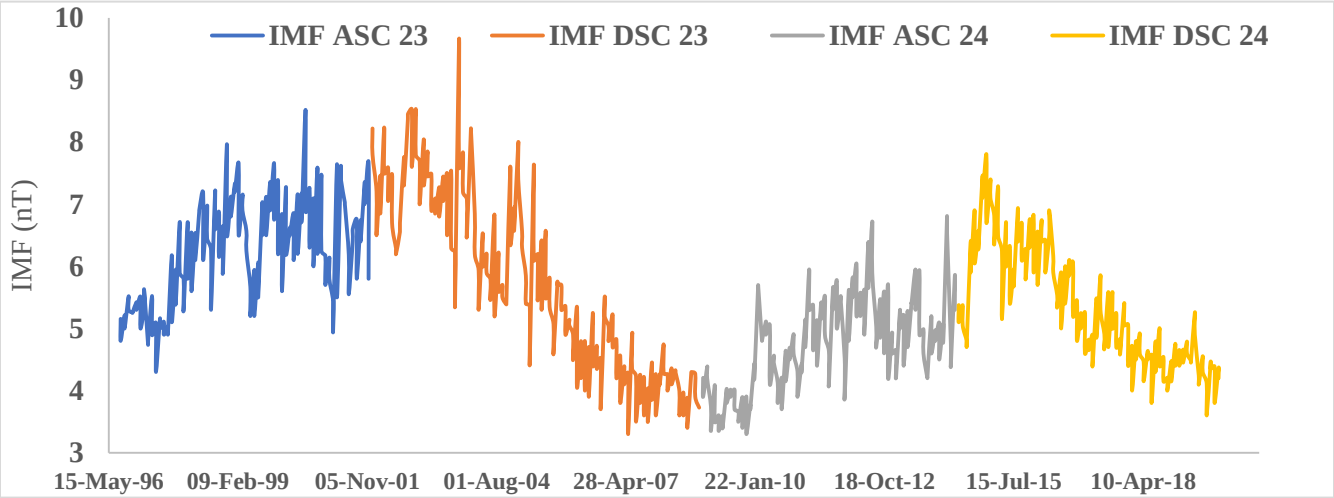

Fig. 5 Time Series Plot of the Monthly Average Values of the IMF Variation for the ASC and DSC Phases of SC 23 and 24

4.2.2. The Monthly Average Solar Wind Parameters Variation for SCs 23 and 24.

Figs 6-8 are the plots of the monthly average values for the ASC and DSC Phases of SCs 23 and 24 for the solar wind parameters (SWS (Fig 6), SWT (Fig 7), and SWPD (Fig 8)). Solar wind parameters during SC 23 and SC 24 were compared as follows: during the ASC phases, SWS was higher during the ASC phase of SC 23 - average values in parentheses - (416.56 km/s) compared to SC 24 (387.98 km/s). SWT was significantly higher in SC 23 during the ASC phase (SC 23 $\times 10^4$ K; SC 24: 6.55 23 $\times 10^4$ K). SWPD was higher during the ASC phase of SC 23 (SC 23: 6.08 N/cm^3; SC 24: 5.07 N/cm^3). During the DSC phases: SWS was higher during the DSC phase of SC 23 (439.01 km/s) compared to SC 24 (417.47 km/s). SWT was higher during the DSC phase of SC 23 (SC 23: 9.64 23 $\times 10^4$ K; SC 24: 8.03 23 $\times 10^4$ K). SWPD was higher during the DSC phase of SC 24 compared to SC 23 (SC 23: 5.13 N/cm^3; SC 24: 6.21 N/cm^3). SWS was higher during SC 23 in both ASC and DSC phases compared to SC 24. SWT was higher during SC 23 in both ASC and DSC phases compared to SC 24. SWPD was higher in the ASC phase of SC 23 but higher in the DSC phase of SC 24. These comparisons indicate that SC 23 generally experienced higher solar wind speeds and temperatures during both phases compared to SC 24, while solar wind plasma density showed varying trends, being higher in SC 23 during the ASC phase but higher in SC 24 during the DSC phase. These differences could reflect varying solar and heliospheric conditions between the two solar cycles. McComas et al., (2013) and Gopalswamy, et al., (2015), examine solar wind characteristics and geomagnetic activity during SCs 23 and 24. The authors find that the solar wind parameters, including speed, density, and

temperature, were generally lower during SC 24, which was the weakest cycle in over a century (see Bothmer et al., 2024).

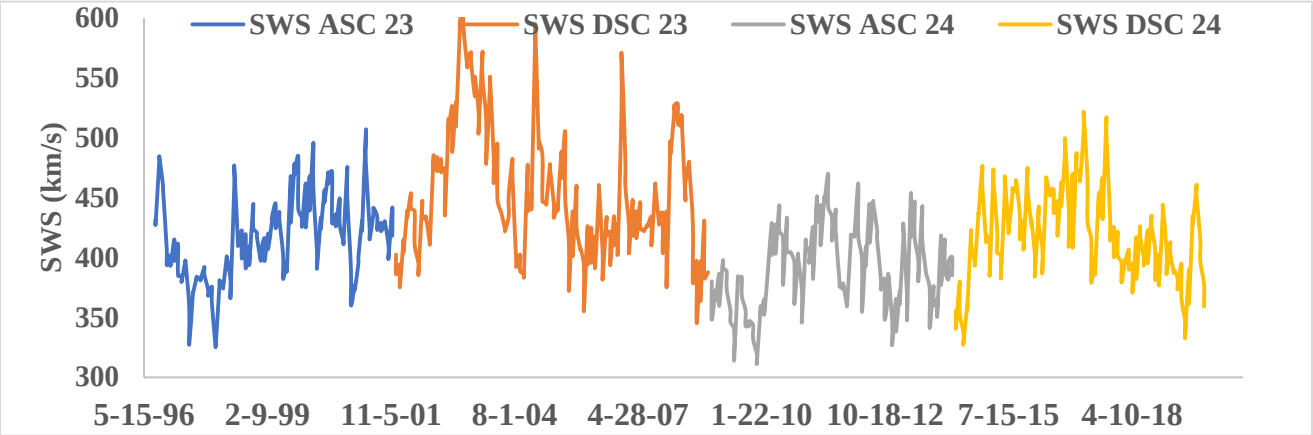

Fig. 6 Time Series Plot of the Monthly Average Values of SWS Variation for the ASC and DSC Phases of SC 23 and 24

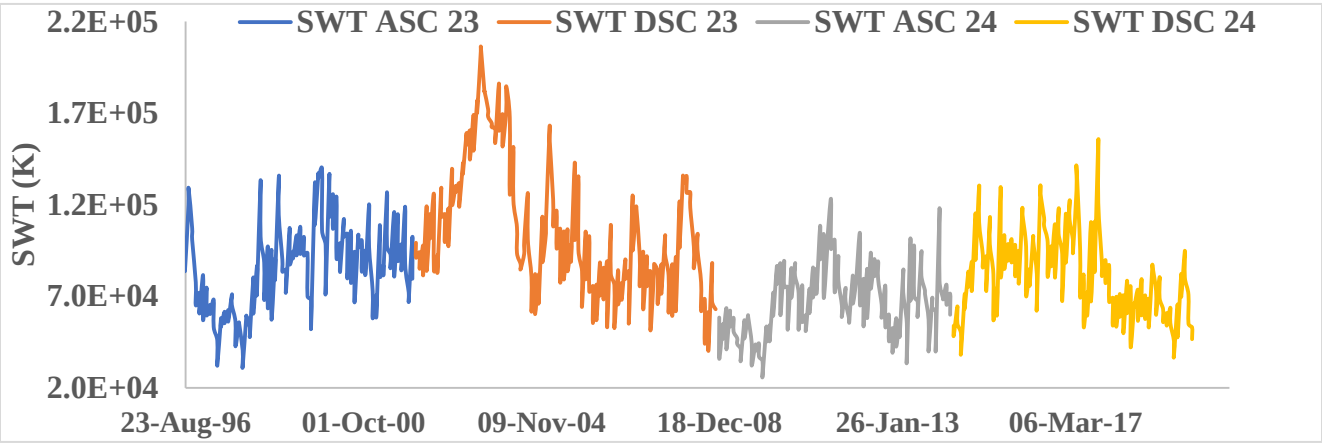

Fig. 7 Time Series Plot of the Monthly Average Values of SWT Variation for the ASC and DSC Phases of SC 23 and 24

Fig. 8 Time Series Plot of the Monthly Average Values of the SWPA Variation for the ASC and DSC Phases of SC 23 and 24

4.2.3. The Monthly Average Geomagnetic Indices Variation for SCs 23 and 24

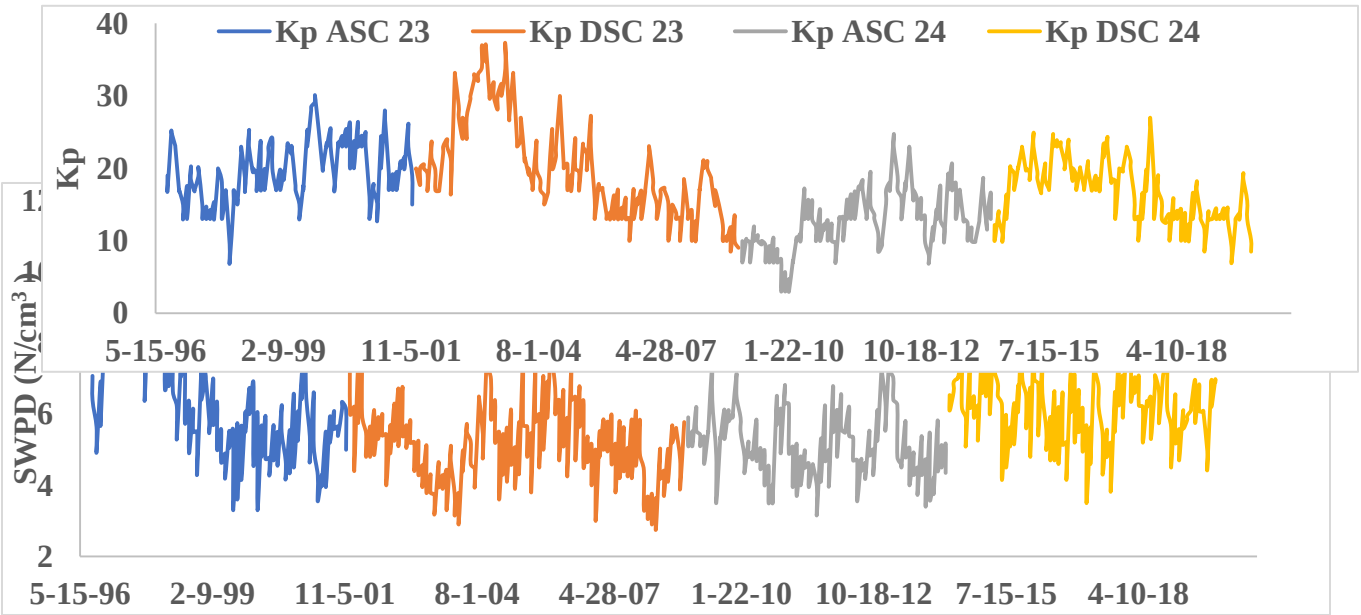

Fig. 9 Time Series Plot of the Monthly Average Values of the Kp Variation for the ASC and DSC Phases of SC 23 and 24

Fig. 10 Time Series Plot of the Monthly Average Values of the Dst Variation for the ASC and DSC Phases of SC 23 and 24

Fig. 11 Time Series Plot of the Monthly Average Values of the ap Variation for the ASC and DSC Phases of SC 23 and 24

For the geomagnetic activity indices (the average monthly plots are shown in Figs 9-11), the Kp index monthly average values were higher during SC 23 than SC 24, they were generally lower during the ASC phase of SC 24 than other phases. The Dst index monthly average values were more negative during SC 23 than SC 24, indicating higher geomagnetic activity, they peaked negatively during high SSN, indicating increased geomagnetic activity during high solar activity.

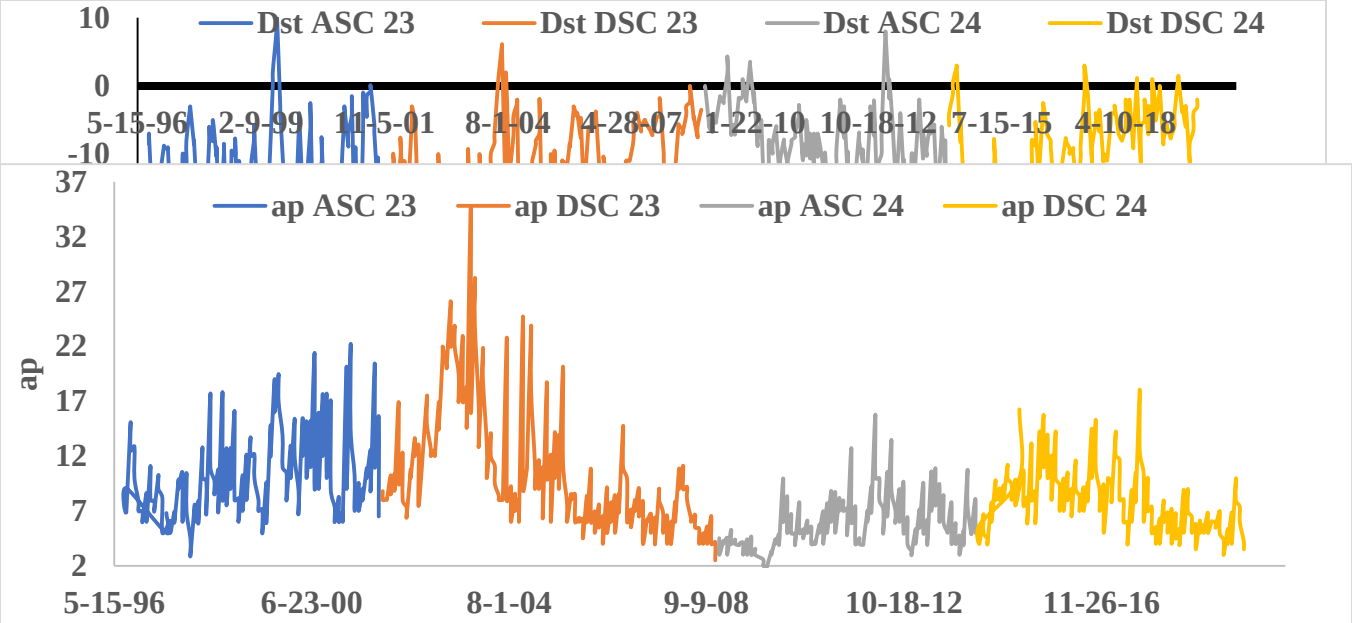

The ap index average monthly values were higher during SC 23 than SC 24, indicating higher geomagnetic activity, and generally, peaks during high SSN values, suggesting more geomagnetic activity during periods of high solar activity. This comprehensive analysis reveals that SC 23 exhibited higher geomagnetic activity, CR intensity differences, and solar-terrestrial parameter variations compared to SC 24, with distinct patterns observed between the ASC and DSC phases in each cycle. Gonzalez et al. (2011) and Tsurutani et al. (2014) showed that geomagnetic indices such as Dst and Kp were generally higher during SC 23 than 24. The study attributes this to the higher solar activity and stronger solar wind parameters during cycle 23 compared to the weaker cycle 24. Kilpua et al. (2015) and Richardson (2013) highlight that during the ascending phase of solar cycle 23, there were more frequent and intense geomagnetic storms compared to solar cycle 24, due to stronger solar wind streams and more frequent CMEs.

Table 1 presents the estimated median and mean values along with the associated standard errors for various parameters analyzed.

- CR Intensity average values showed similar values during the ASC and DSC phases of each SC and were higher during SC 24 than SC 23.

- SSN average values indicate higher during the ASC phase than the DSC phase for both SCs and were higher during SC 23 than SC 24.
- IMF average values showed higher values during the ASC phase of SC 23, and lowest during the ASC phase of SC 24.
- SWS and SWT average values were higher during the DSC phase of each SC than during the ASC phase, they were also higher during SC 23 than SC 24.
- SWPD average values were higher during the ASC phase than the DSC phase. SWPD values did not follow any specific trend relative to the SSN cycle.
- Geomagnetic Indices (Kp, Dst, ap) average values generally have higher positive or negative values during SC 23 than SC 24, also, the average values indicate that high geomagnetic activities correlate with high solar activities, as measured by SSN

Table 1a Central Tendency Values Estimate of the Parameters of the ASC and the DSC Phases of SC 23 and 24

Parameter	ASC 23	DSC 23	ASC 24	DSC 24
Median Values				
CR ($x10^7$)	1.86	1.88	1.96	1.98
SSN	115.74	46.53	60.61	24.25
IMF (nT)	6.23	5.51	4.73	5.08
SWS	416.56	439.01	387.98	417.47
SWT($x10^4$) K	8.53	9.64	6.55	8.03
SWPD (N/cm^3)	6.08	5.13	5.07	6.21
Kp	19.58	18.51	13.01	17.01
Dst	-14.01	-11.37	-7.42	-8.13
ap	9.32	8.58	5.01	7.62

Table 1b Central Tendency Values Estimate of the Parameters of the ASC and the DSC Phases of SC 23 and 24

Parameter	ASC 23	DSC 23	ASC 24	DSC 24
Mean Values with Associated Standard Errors				
CR($x10^7$)	1.85±0.36	1.88±0.53	1.96±0.24	1.97±0.28
SSN	109.40±57.11	60.41±45.12	60.27±38.55	37.04±30.49
IMF (nT)	6.24±0.73	5.73±1.25	4.76±0.63	5.33±0.81
SWS	416.23±28.23	453.75±44.81	390.58±28.53	419.48±31.39
SWT($x10^4$) K	8.57±1.99	10.61±2.91	6.68±1.55	8.16±1.88
SWPD (N/cm^3)	6.33±1.29	5.18±0.91	5.16±0.76	6.19±0.79
Kp	19.74±3.55	19.96±5.42	12.72±3.27	16.80±3.63
Dst	-14.35±7.57	-13.33±7.39	-8.10±4.65	-9.75±5.96
ap	10.28±3.16	10.15±4.41	5.86±1.92	7.94±2.32

4.3 Monthly Average Distribution Plots

The plots of the monthly average distribution for CR, SSN, IMF, solar wind parameters (SWS, SWT, SWPD), and geomagnetic activity indices (Kp, Dst, ap) for the ASC and the DSC phases of SC 23 and 24 are shown in Figs 12-20. the kurtosis and the skewness of the distributions are shown in Table 2 for each phase.

Table 2: Value of Skewness and Kurtosis for The Distribution Plots Using The Monthly Average Values for the ASC and DSC phases of SCs 23 and 24

	ASC 23	ASC 23	DSC 23	DSC 23	ASC 24	ASC 24	DSC 24	DSC 24
	skewness	kurtosis	skewness	kurtosis	skewness	kurtosis	skewness	kurtosis
CR	-1.24	2.99	-0.24	-0.98	0.23	-0.96	-0.76	-0.53
SSN	0.03	-1.00	0.99	0.05	0.08	-1.29	0.82	-0.44
IMF	0.03	-0.80	0.28	-0.99	0.21	-0.37	0.49	-0.72
SWS	0.06	-0.03	0.75	0.07	0.04	-0.64	0.13	-0.18
SWT	0.18	-0.51	0.69	-0.19	0.39	-0.11	0.55	-0.04
SWPD	0.43	-0.39	0.46	0.46	0.38	-0.15	-0.03	0.06
Dst	-1.06	1.70	-0.73	0.60	-0.60	1.82	-0.47	-0.56
Kp	-0.02	-0.28	0.68	-0.26	0.23	0.11	0.06	-0.75
ap	0.93	0.35	1.41	1.86	1.18	1.80	0.87	0.76

4.3.1 Distribution Plot of CR Variations for the ASC and DSC Phases of SCs 23 and 24

The analysis of the distribution plot of CR intensity during the ASC and DSC phases of SCs 23 and 24 reveals distinct statistical characteristics in their distributions shown in Fig 12. For the ASC phase of SC 23, the distribution is negatively skewed and leptokurtic, indicating a long-left tail and a higher propensity for extreme values due to heavier tails and a sharper peak compared to a normal distribution. This suggests greater variability and more pronounced CR intensity fluctuations during this period. In contrast, the DSC phase of SC 23 shows a slightly negatively skewed but more symmetric and platykurtic distribution, implying fewer extreme values, a more uniform spread, and a flatter peak, signaling more stability in CR intensity during this phase. For SC 24, the ASC phase presents a slightly positively skewed and platykurtic distribution, meaning a smaller right tail with fewer extreme values and a more balanced, evenly spread pattern. Meanwhile, the DSC phase of SC 24 is negatively skewed and platykurtic, indicating a longer left tail with fewer outliers and a generally uniform spread of CR intensities.

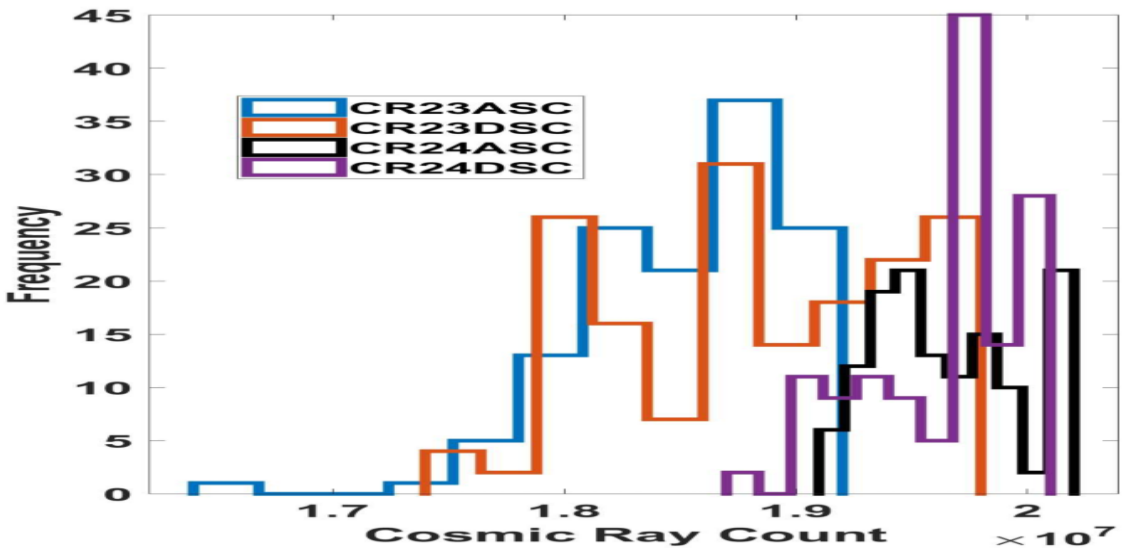

Fig. 12: Distribution Plot Using the Monthly Average Values of CR Intensity Variations for the ASC and DSC Phases of SCs 23 and 24

These findings show that the ASC phase of SC 24 has a nearly symmetric distribution, with a slight tendency toward higher values, whereas the DSC phase has lower values with fewer extreme variations but remains evenly distributed. This comparison between SC 23 and SC 24 highlights the differences in monthly average CR intensity variations, particularly in how solar modulation is influenced by solar wind conditions and magnetic fields, and impacts CR propagation differently during the ASC and DSC phases (Moraal & McCracken, 2012; Potgieter, 2013; Ahluwalia & Ygbuhay, 2014; Aslam & Badruddin, 2015). Further studies by Heber et al. (2009), Kuwabara et al. (2009), and Gieseler et al. (2017) explain that solar magnetic field changes, solar wind speed, and the tilt angle of the heliospheric current sheet during different solar cycle phases affect CR modulation. The reversal of the Sun's magnetic field near the solar cycle peak significantly influences cosmic ray propagation during the ASC and DSC phases, leading to the observed differences in CR distribution and intensity.

4.3.2 Distribution Plot of SSN Variations for the ASC and DSC Phases of SCs 23 and 24

The SSN distribution in different SC 23 and 24 phases shows (shown in Fig 13) that ASC phases are almost symmetrical with a slight right skew, suggesting balanced distributions around the mean. The distributions are platykurtic, especially in SC 24, indicating fewer extreme values. The DSC phases of both cycles are moderately right-skewed, indicating a predominance of lower values with a tendency towards higher values. Overall, the ASC phases of both cycles show nearly symmetrical and flatter distributions, while the DSC phases are moderately right-skewed

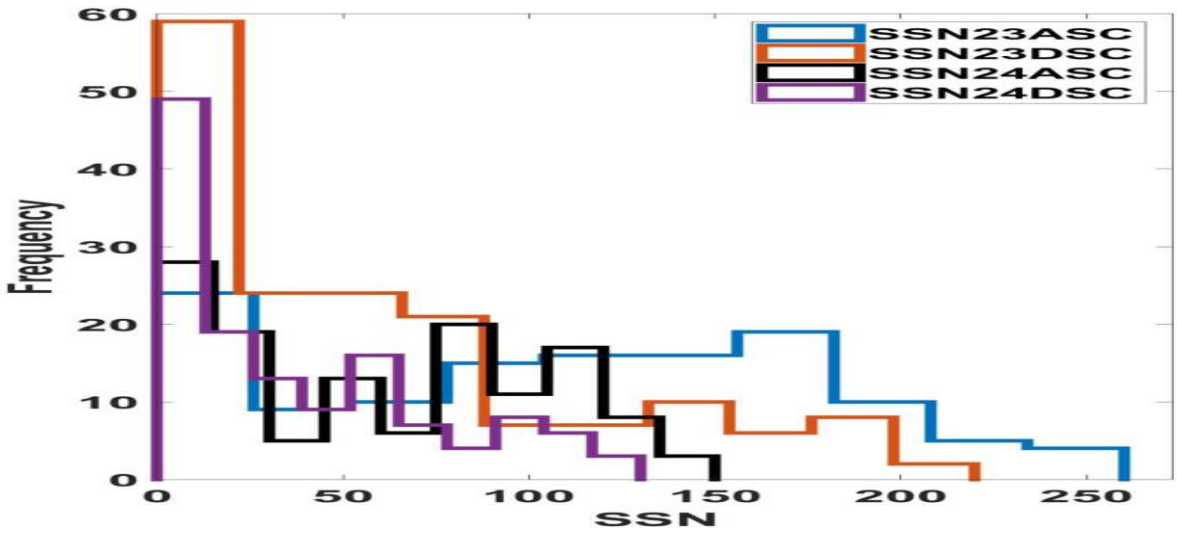

with tail behaviors closer to normal but slightly platykurtic in SC 24. During the DSC phase of a SC, the SSNs typically decline gradually. This extended period of lower sunspot numbers would mean more frequent occurrences of low values. The DSC phases of SCs are right-skewed due to extended periods of lower SSN during the declining phase. Research by Abha et al. (2024) discusses how sunspot group dynamics, including flare activity and magnetic complexity, differ across phases and SCs, further explaining the variability in SSN distributions. Additional studies, such as those by Hathaway and Upton (2014) and Iwok (2011), also corroborate the distinct distribution behaviors seen between the ASC and DSC phases of SCs 23 and 24.

Fig. 13 Distribution Plot Using the Monthly Average Values of SSN Variations for the ASC and DSC Phases of SCs 23 and 24

4.3.3 Distribution Plot of IMF Variations for the ASC and DSC Phases of SCs 23 and 24

The distribution of the IMF for the ASC and DSC phases of SC 23 and SC 24, as depicted in Fig 14, shows a slightly right-skewed and moderately platykurtic ASC Phase, indicating mild asymmetry with more frequent lower values and a somewhat flatter shape compared to a normal distribution. The DSC Phase is moderately right-skewed and slightly platykurtic, displaying more noticeable asymmetry with more frequent lower values and a longer tail towards higher values. Both ASC phases (SC 23 and SC 24) exhibit slight right skewness, with SC 23 being almost symmetrical and platykurtic, indicating flatter distributions with fewer extreme values. Both DSC phases show right skewness, with SC 24 having a higher skewness value, indicating more pronounced asymmetry. Both phases are platykurtic, with SC 23 being more so, indicating fewer extreme values than SC 24. This analysis highlights the differences in distribution shapes between the ASC and DSC phases of SCs 23 and 24, particularly in terms of symmetry and tail

behavior. The Sun is the source of IMF, any changes in the Sun magnetic field patterns will manifest in the recorded values of IMF. Upton et al., (2021), reported variations in the meridional flow, which were more pronounced in SC 23 than in the weaker SC 24

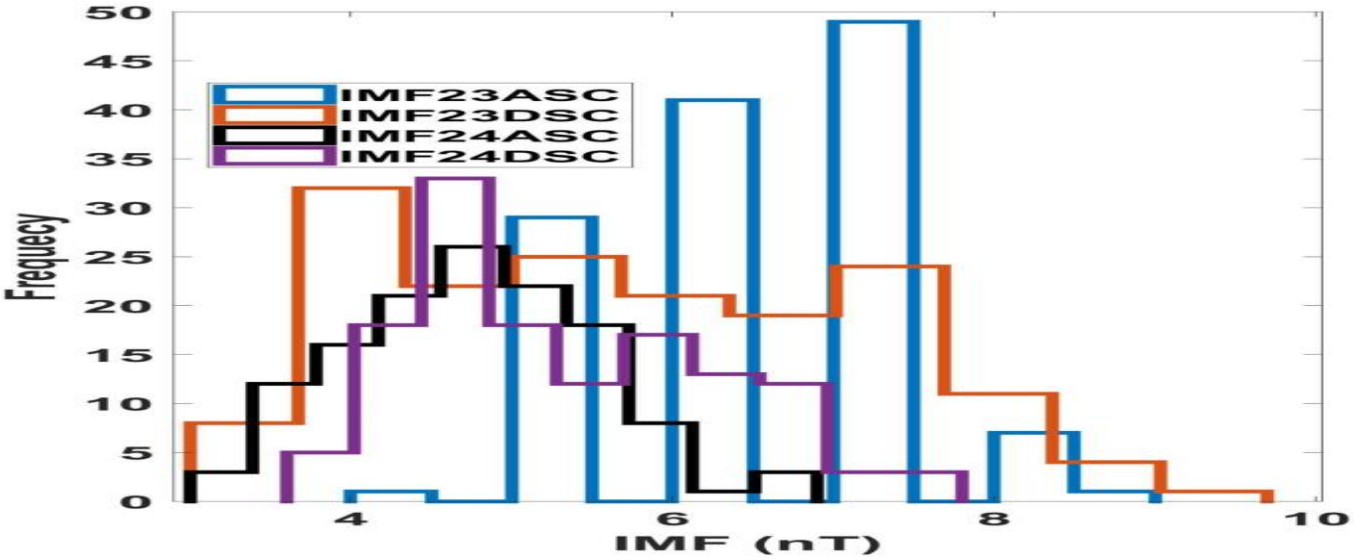

Fig. 11 Distribution Plot Using the Monthly Average Values of IMF Variations for the ASC and DSC Phases of SCs 23 and 24

4.3.4 Distribution Plot of SWS Variations for the ASC and DSC Phases of SCs 23 and 24

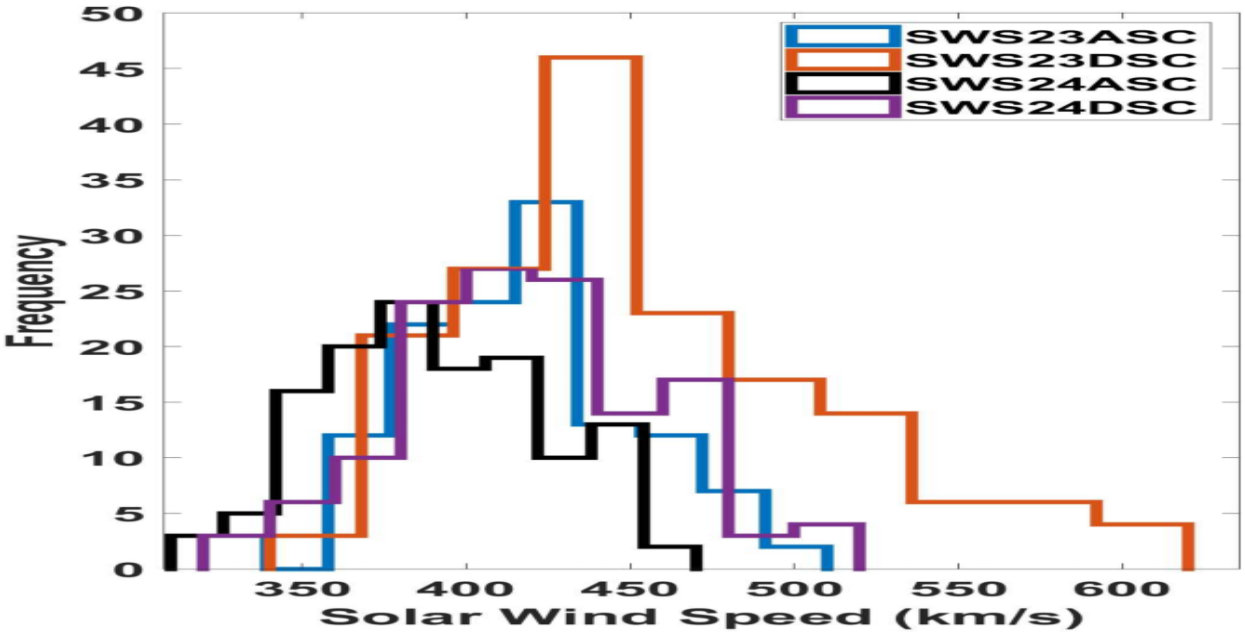

Fig. 15 Distribution Plot Using the Monthly Average Values of SWS Variations for the ASC and DSC Phases of SCs 23 and 24

The SWS distribution during the ASC phase of SC 23 (given in Fig 15) is almost perfectly symmetrical, while the DSC phase of SC 23 is moderately skewed to the right. The ASC phase of SC 24 also shows an almost perfectly symmetrical distribution, while the DSC phase has a slight right skew. Both ASC phases are close to mesokurtic, while the DSC phases are slightly platykurtic. This comparison highlights the differences in symmetry and tail behavior between the ASC and DSC phases of SCs 23 and 24, indicating variations in SWS distribution characteristics. Studies on the statistical distribution of CME and solar wind speeds provide insight into how these phases exhibit distinct patterns in terms of symmetry and kurtosis, with ASC phases being closer to mesokurtic and DSC phases slightly platykurtic (Zhang et al., 2021; Echer et al., 2023; Mishra et al., 2024), these conclusions were similar to ours.

4.3.5 Distribution Plot of SWT Variations for the ASC and DSC Phases of SCs 23 and 24

The analysis of Fig 16 which is the distribution plot using the monthly average values of SWT variations for the ASC and DSC phases of SCs 23 and 24 indicates that for the SC 23 ASC phase, the SWT distribution displays a slight right skew, signifying a mild asymmetry with a tendency towards higher values. The distribution is also platykurtic, indicating that it is flatter than a normal distribution with fewer extreme values. In the case of the SC 23 DSC phase, the distribution is moderately skewed to the right, suggesting more frequent lower values and a tail extending towards higher values. It is also slightly platykurtic, signifying that it is somewhat flatter than a normal distribution. Moreover, the ASC phase of SC 24 exhibited a distribution that is more skewed to the right than the ASC phase of SC 23, demonstrating a greater tendency towards higher values, and slight platykurtic characteristics, close to mesokurtic, indicating tails similar to a normal distribution but slightly flatter. Similarly, the DSC phase of SC 24 distribution is moderately skewed to the right, indicating an asymmetry with more frequent lower values and a tail towards higher values. It is slightly platykurtic, indicating that it is flatter than a normal distribution but closer to mesokurtic compared to the DSC phase of SC 23.

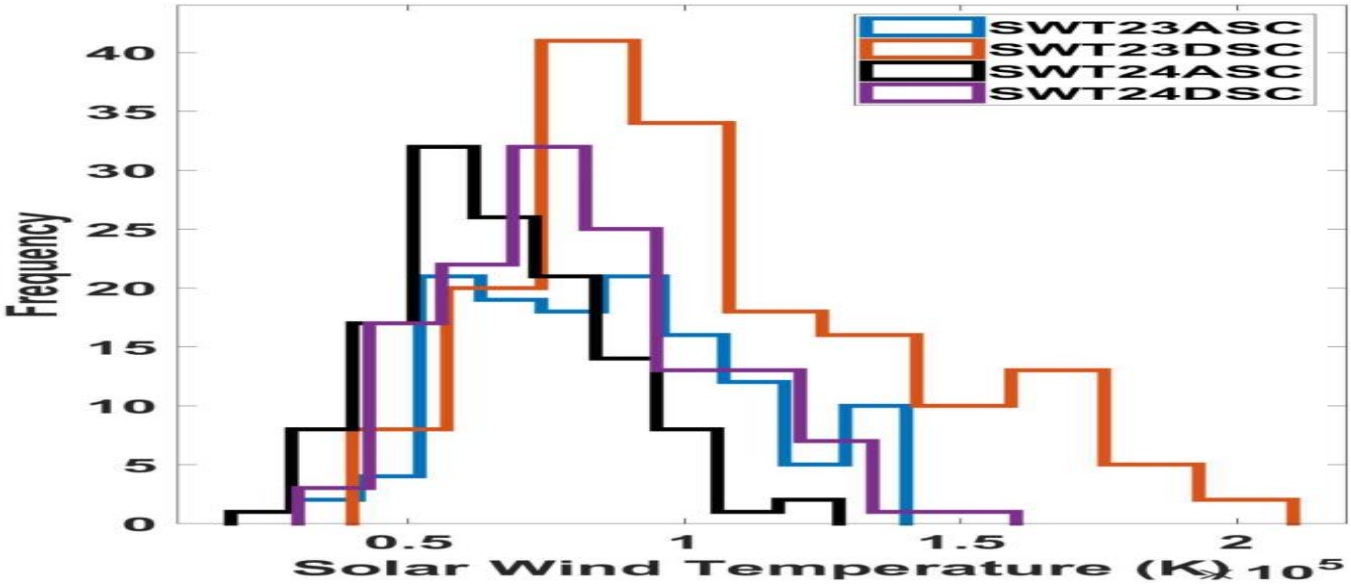

Fig. 16 Distribution Plot Using the Monthly Average Values of SWT Variations for the ASC and DSC Phases of SCs 23 and 24

In summary, during the ASC phases, both cycles have slightly right-skewed distributions, with SC 24 being more skewed and less flat (less platykurtic) than SC 23. During the DSC phases, both cycles exhibit moderate right skewness, with SC 23 having a more pronounced skew and flatter distribution compared to SC 24. This comparison emphasizes symmetry and tail behavior between the ASC and DSC phases of SCs 23 and 24, revealing differences in the distribution of SWT. The works by White et al., (2011), Gopalswamy et al. (2012), Zhang et al., (2021), and other researchers used microwave observations and magnetic field data to support the idea that the solar wind properties, including SWT, display different behaviors during the ASC and DSC phases of SCs 23 and 24. They observed notable differences in solar activity during these phases, including the presence of skewness in solar wind parameters due to solar events CMEs, which are more frequent in the ASC phase, contributing to the right skew. Further, research examining solar minimum periods between cycles 23 and 24 noted variations in solar irradiance and solar wind characteristics, which ties into your description of kurtosis, where distributions tend to be flatter during quieter periods and exhibit more pronounced tails during higher solar activity.

4.3.6 Distribution Plot of SWPD Variations for the ASC and DSC Phases of SCs 23 and 24

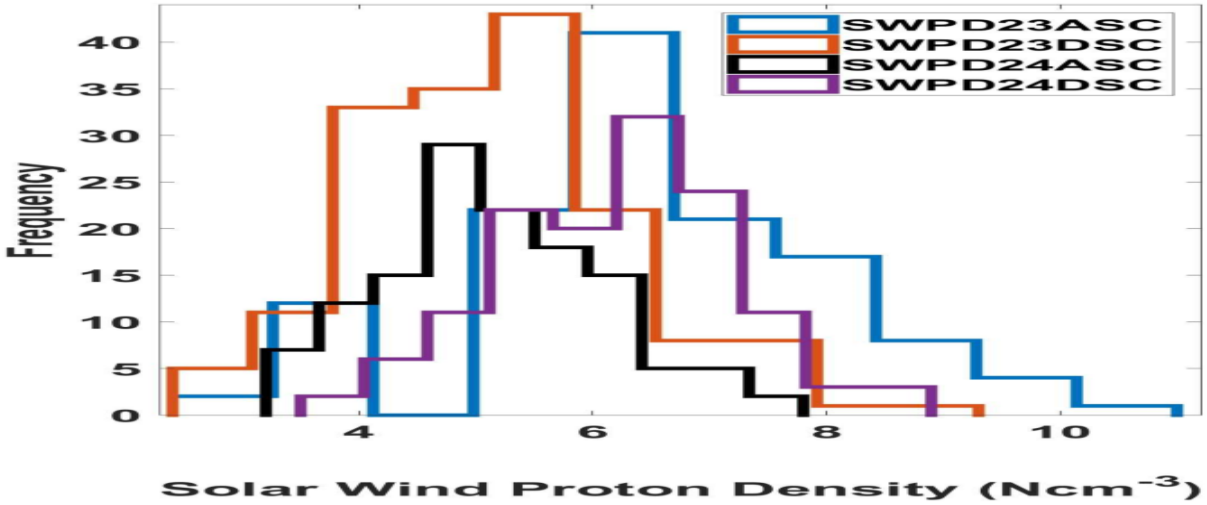

Fig. 17 Distribution Plot Using the Monthly Average Values of SWPD Variations for the ASC and DSC Phases of SCs 23 and 24

The SWPD distribution shown in Fig 17 for the ASC phase of SC 23 is moderately skewed to the right, with a tendency for more frequent lower values and a tail extending towards higher values. The DSC phase of SC 23 shows similar right skewness and is also leptokurtic, indicating a more peaked distribution with heavier tails. The ASC phase of SC 24 has a slightly skewed right distribution, while the DSC phase of SC 24 is almost symmetrical. In summary, both cycles show moderate right skewness during their ASC phases, but the DSC phases exhibit different distribution shapes, with SC 23 being leptokurtic and SC 24 being closer to mesokurtic.

4.3.6 Distribution Plots of Geomagnetic Indices Variations for the ASC and DSC Phases of SCs 23 and 24

The analysis of the distributions of the Kp, Dst, and ap indices (shown in Figs 18-20) during the SCs 23 and 24 phases can be supported by several studies that analyze the geomagnetic and solar activity. For instance, the Kp index distribution during SC 23's ASC and DSC phases shows differences in symmetry and tail behavior, which correlate with the frequency and intensity of geomagnetic events. Research reveals that during the ASC of SC 23, the distribution is nearly symmetrical and slightly platykurtic, indicating a flatter-than-normal spread with fewer extreme values (Rangarajan & Lyemori, 1997).

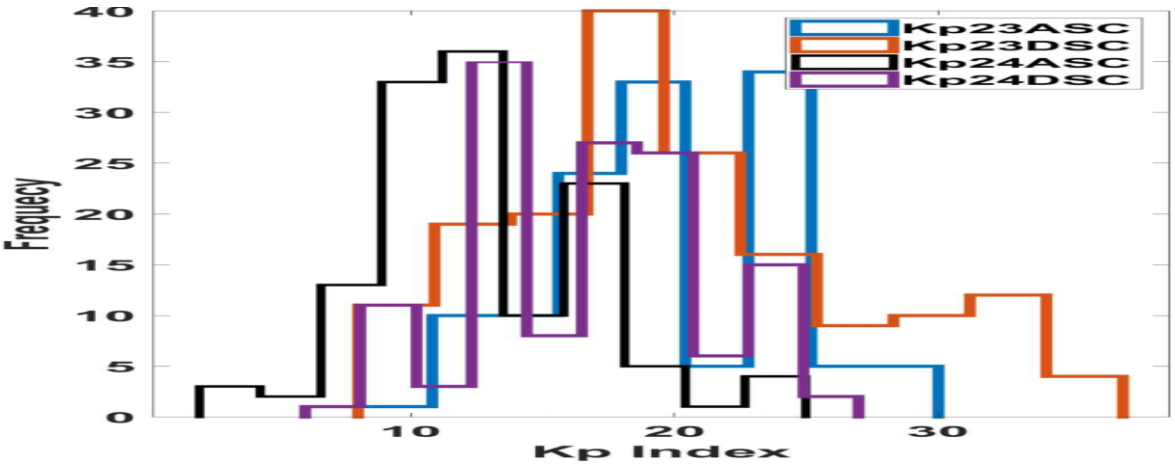

Fig. 18 Distribution Plot Using the Monthly Average Values of Kp Variations for the ASC and DSC Phases of SCs 23 and 24

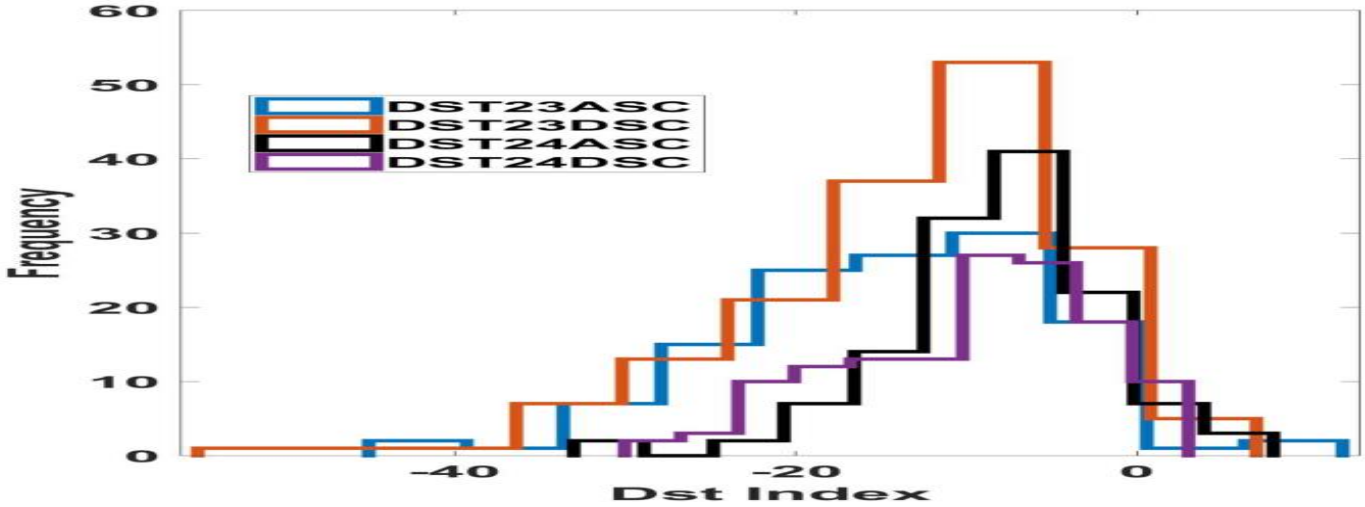

Fig. 19 Distribution Plot Using the Monthly Average Values of Dst Variations for the ASC and DSC Phases of SCs 23 and 24

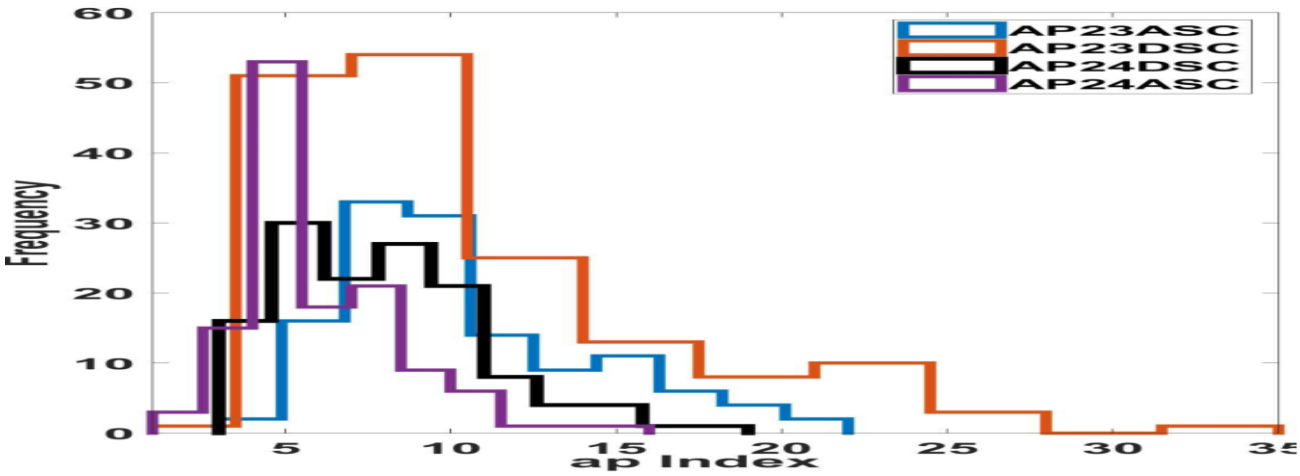

Fig. 20 Distribution Plot Using the Monthly Average Values of ap Variations for the ASC and DSC Phases of SCs 23 and 24

Similarly, during SC 23's DSC phase, a moderate right skew is observed, highlighting a tail towards higher values, while SC 24 shows a similar but less pronounced distribution.

For the Dst index, studies indicate that during the ASC phase of SC 23, a negative skewness with leptokurtic characteristics is present, suggesting extreme values and heavy tails, signifying intense geomagnetic storms. This pattern is less extreme in SC 24, where fewer negative extreme values and a more normal-like distribution are observed, particularly in the DSC phase.

Lastly, the ap index distribution shows significant differences in right skewness and kurtosis between the two solar cycles. During SC 23's DSC phase, a pronounced right skew and leptokurtic behavior highlight frequent extreme values and a long tail towards higher values. In contrast, SC 24 exhibits less extreme but still noticeable right skewness. These variations in skewness and kurtosis provide insights into the intensity and frequency of geomagnetic storms, with SC 23 showing more extreme behavior than SC 24, especially during the DSC phases. These observations are crucial for understanding space weather patterns and the impact of solar activity on geomagnetic indices across different solar cycles.

4.4 Regression Analysis

Table.3: Correlation Coefficient Amongst the Studied Parameter

parameter	ASC 23	DSC 23	ASC 24	DSC 24
CR/SSN	-0.55	-0.79	-0.71	-0.68
CR/IMF	-0.42	-0.88	-0.69	-0.77
CR/SWT	-0.41	-0.66	-0.54	-0.26
CR/SWPD	0.46	0.01	0.27	-0.12
CR/SWS	-0.39	-0.46	-0.47	-0.08
CR/Kp	-0.38	-0.80	-0.68	-0.46
CR/Dst	0.01	-0.51	-0.50	-0.49
CR/ap	-0.33	-0.69	-0.51	-0.34

Table 4: Linear Regression Fits to the Logarithm Values of the Studied Parameters

SC	ASC	DSC
SC 23	$\log \mathrm{CR} = -(0.01 \pm 0.01) \log \mathrm{SSN} + 7.29$	$\log \mathrm{CR} = -(0.02 \pm 0.01) \log \mathrm{SSN} + 7.31$
SC 24	$\log \mathrm{CR} = -(0.01 \pm 0.01) \log \mathrm{SSN} + 7.31$	$\log \mathrm{CR} = -(0.01 \pm 0.01) \log \mathrm{SSN} + 7.31$
SC 23	$\log \mathrm{CR} = -(0.07 \pm 0.01) \log \mathrm{IMF} + 7.33$	$\log \mathrm{CR} = -(0.11 \pm 0.01) \log \mathrm{IMF} + 7.36$
SC 24	$\log \mathrm{CR} = -(0.06 \pm 0.01) \log \mathrm{IMF} + 7.34$	$\log \mathrm{CR} = -(0.07 \pm 0.01) \log \mathrm{IMF} + 7.35$
SC 23	$\log \mathrm{CR} = -(0.03 \pm 0.01) \log \mathrm{SWT} + 7.43$	$\log \mathrm{CR} = -(0.07 \pm 0.01) \log \mathrm{SWT} + 7.61$
SC 24	$\log \mathrm{CR} = -(0.03 \pm 0.01) \log \mathrm{SWT} + 7.42$	$\log \mathrm{CR} = -(0.02 \pm 0.01) \log \mathrm{SWT} + 7.37$
SC 23	$\log \mathrm{CR} = (0.04 \pm 0.01) \log \mathrm{SWPD} + 7.23$	$\log \mathrm{CR} = (0.01 \pm 0.01) \log \mathrm{SWPD} + 7.28$
SC 24	$\log \mathrm{CR} = (0.02 \pm 0.01) \log \mathrm{SWPD} + 7.28$	$\log \mathrm{CR} = -(0.01 \pm 0.01) \log \mathrm{SWPD} + 7.31$
SC 23	$\log \mathrm{CR} = -(0.11 \pm 0.01) \log \mathrm{SWS} + 7.56$	$\log \mathrm{CR} = -(0.13 \pm 0.01) \log \mathrm{SWS} + 7.62$
SC 24	$\log \mathrm{CR} = -(0.08 \pm 0.01) \log \mathrm{SWS} + 7.51$	$\log \mathrm{CR} = -(0.01 \pm 0.01) \log \mathrm{SWS} + 7.33$
SC 23	$\log \mathrm{CR} = -(0.04 \pm 0.01) \log \mathrm{Kp} + 7.32$	$\log \mathrm{CR} = -(0.08 \pm 0.01) \log \mathrm{Kp} + 7.38$
SC 24	$\log \mathrm{CR} = -(0.03 \pm 0.01) \log \mathrm{Kp} + 7.32$	$\log \mathrm{CR} = -(0.03 \pm 0.01) \log \mathrm{Kp} + 7.33$
SC 23	$\log \mathrm{CR} = (0.01 \pm 0.01) \log\lvert\mathrm{Dst}\rvert + 7.27$	$\log \mathrm{CR} = -(0.02 \pm 0.01) \log\lvert\mathrm{Dst}\rvert + 7.31$
SC 24	$\log \mathrm{CR} = -(0.01 \pm 0.01) \log\lvert\mathrm{Dst}\rvert + 7.31$	$\log \mathrm{CR} = -(0.01 \pm 0.01) \log\lvert\mathrm{Dst}\rvert + 7.31$

SC 23	$\log CR = -(0.02 \pm 0.01) \log ap + 7.29$	$\log CR = -(0.05 \pm 0.01) \log ap + 7.32$
SC 24	$\log CR = -(0.02 \pm 0.01) \log ap + 7.31$	$\log CR = -(0.02 \pm 0.01) \log ap + 7.31$

Table 3 displays the correlation coefficients and in Table 4, the results of log-log fit to the monthly average values of the studied parameters, while the log-log plots of CR intensity against SSN, IMF, SWS, SWT, SWPD, and the geomagnetic indices (Kp, Dst, ap) are shown in Figs 21-

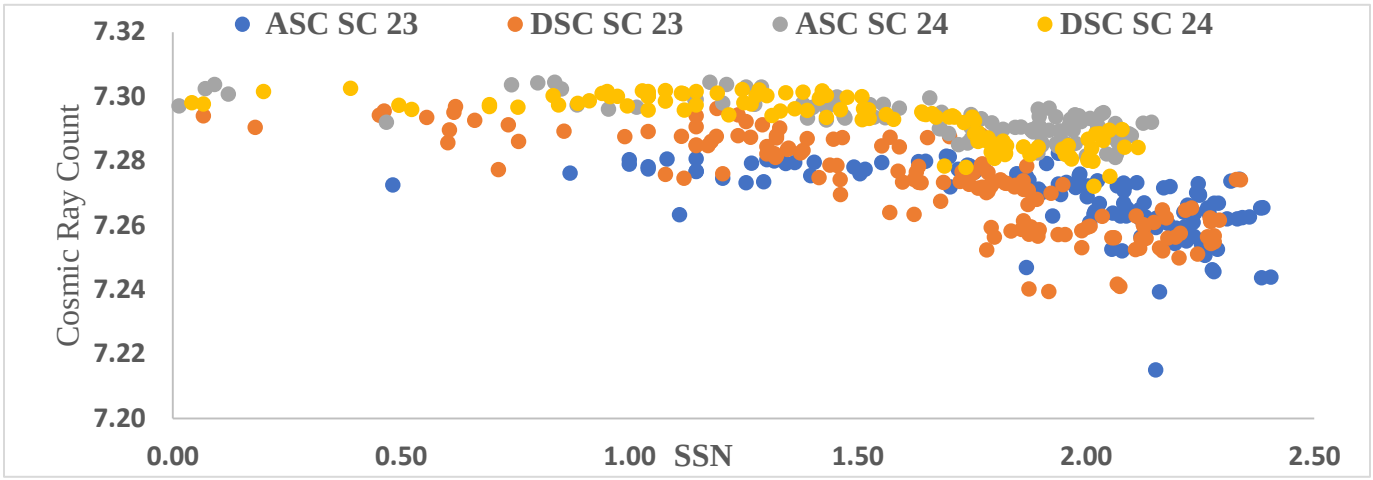

28.

Fig 21: log-log Plot of the Monthly Average Values of Cosmic Ray Intensity vs Sunspot Number for the ASC and the DSC Phases of SC 23 and 24

Fig 21 is the log-log Plot of the Monthly Average Values of Cosmic Ray Intensity vs Sunspot Number for the ASC and the DSC Phases of SC 23 and 24**.** The plots and the results in Tables 3 and 4 suggest that for CR and SSN variation, the overall relationship patterns are consistent (negative correlations) for both the ASC and DSC phases of SC 23 and 24. SC 23 exhibited a slightly stronger and more pronounced relationship between CRs and SSNs compared to SC 24. During the ASC phase of SC 23 and SC 24, Table 3 shows that both have a similar slope, indicating a similar relationship between CR and SSN. In the DSC phase, SC 23's slope is slightly steeper than SC 24's, suggesting a stronger negative correlation between CR and SSN. Despite these differences, the intercepts are very close, suggesting similar overall CR intensity levels across both solar cycles.

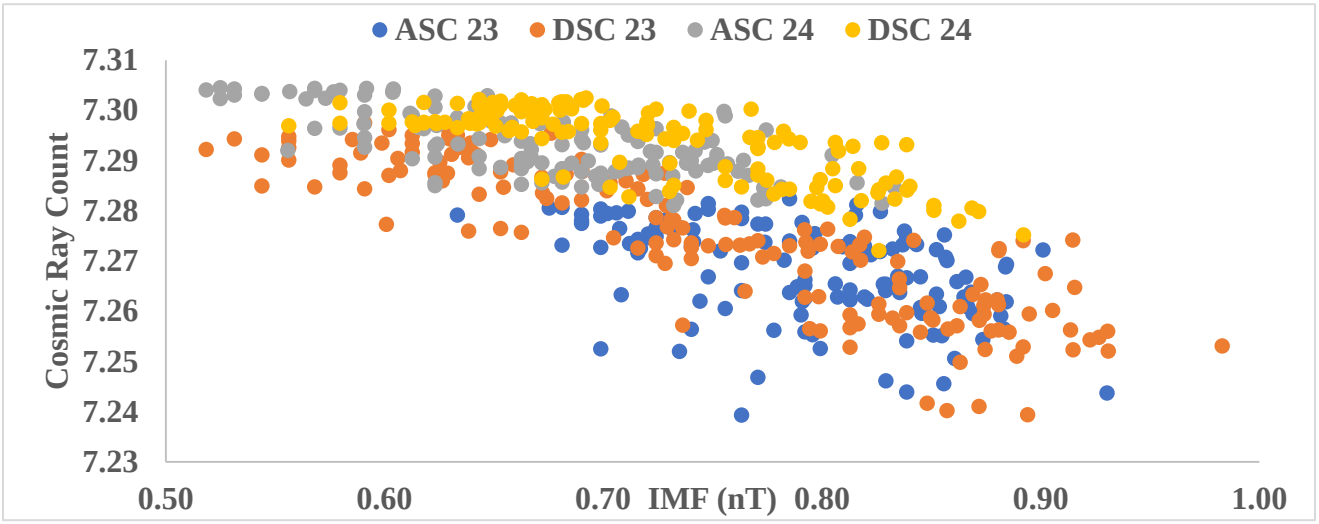

Fig 22: log-log Plot of the Monthly Average Values of the Cosmic Ray Intensity vs IMF for the ASC and the DSC Phases of SC 23 and 24

Fig 22 is the log-log Plot of the Monthly Average Values of Cosmic Ray Intensity vs IMF for the ASC and the DSC Phases of SC 23 and 24. The linear fit indicates that the relationship between CR intensity and IMF is stronger in SC 23 compared to SC 24. The CR intensity is more sensitive to changes in IMF during the ASC and DSC phases of SC 23, with the steepest decline observed during the DSC phase. The baseline CR intensity remains fairly consistent across the different phases and cycles.

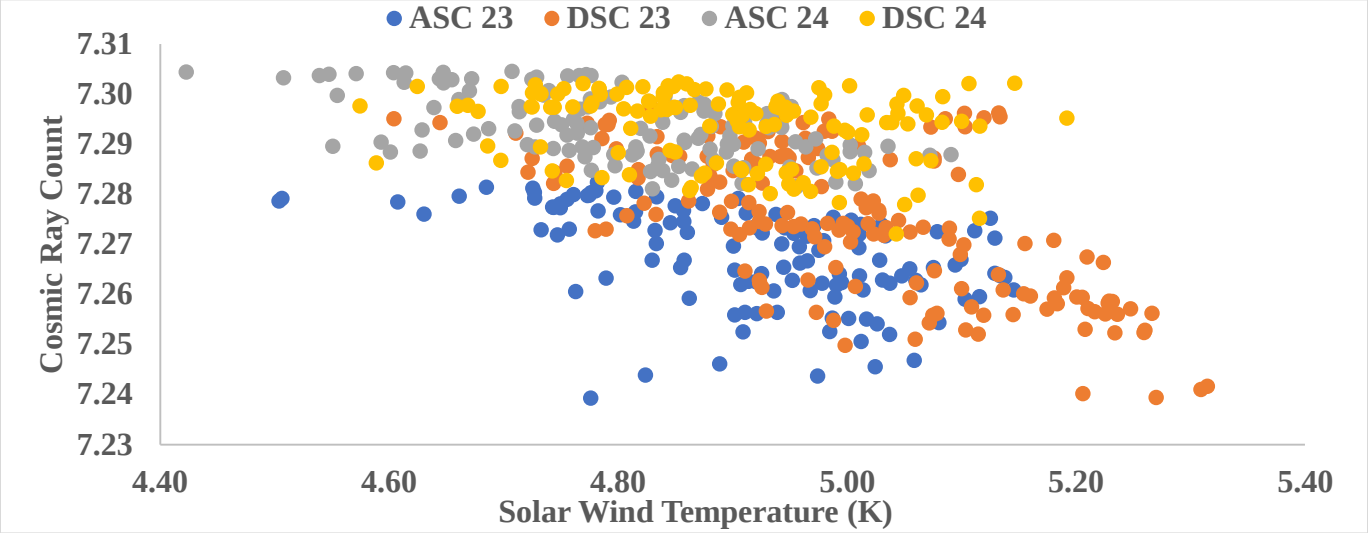

Fig 23: log-log Plot of the Monthly Average Values of the Cosmic Ray Intensity vs SWT for the ASC and the DSC Phases of SC 23 and 24

Fig 23 is the log-log Plot of the Monthly Average Values of Cosmic Ray Intensity vs SWT for the ASC and the DSC Phases of SC 23 and 24. The comparison of linear fits between CR intensity and SWT during the ASC and DSC phases of SCs 23 and 24 (Fig 23, Tables 3 and 4) reveals that both SCs have the same slope of -0.03 with the same uncertainty (0.01). SC 23 has a steeper slope (-0.07) compared to SC 24 (−0.02) during the DSC phase, indicating a much stronger inverse relationship. The DSC phase in SC 23 shows a particularly strong inverse relationship (-0.07) between CR and SWT, suggesting that CR intensity is more sensitive to changes in SWT during this phase. The ASC phases of both SCs have identical slopes and very similar intercepts, indicating a consistent inverse relationship between CR and SWT. In summary, the relationship between cosmic ray intensity and solar wind turbulence shows a significantly stronger inverse correlation during the DSC phase of SC 23 compared to SC 24, while the ASC phases are remarkably consistent across both cycles.

Fig 24 is the log-log Plot of the Monthly Average Values of Cosmic Ray Intensity vs SWPD for the ASC and the DSC Phases of SC 23 and 24. The relationships between CR intensity and SWPD during the ASC and DSC phases of SCs 23 and 24 show that the ASC phase of SC 23 indicates a moderate positive correlation between CR and SWPD. As SWPD increases, CR increases moderately. During the DSC of SC 23, the result shows a weak positive correlation, and the CR is almost independent of SWPD during this phase. The ASC phase of SC 24 indicates

a slight positive correlation, while the DSC phase of SC 24 shows a slight negative correlation. The intercepts are similar across all phases and cycles, with slight variations. The ASC phase of SC 23 shows the highest sensitivity to SWPD, followed by the ASC phase of SC 24. Both DSC

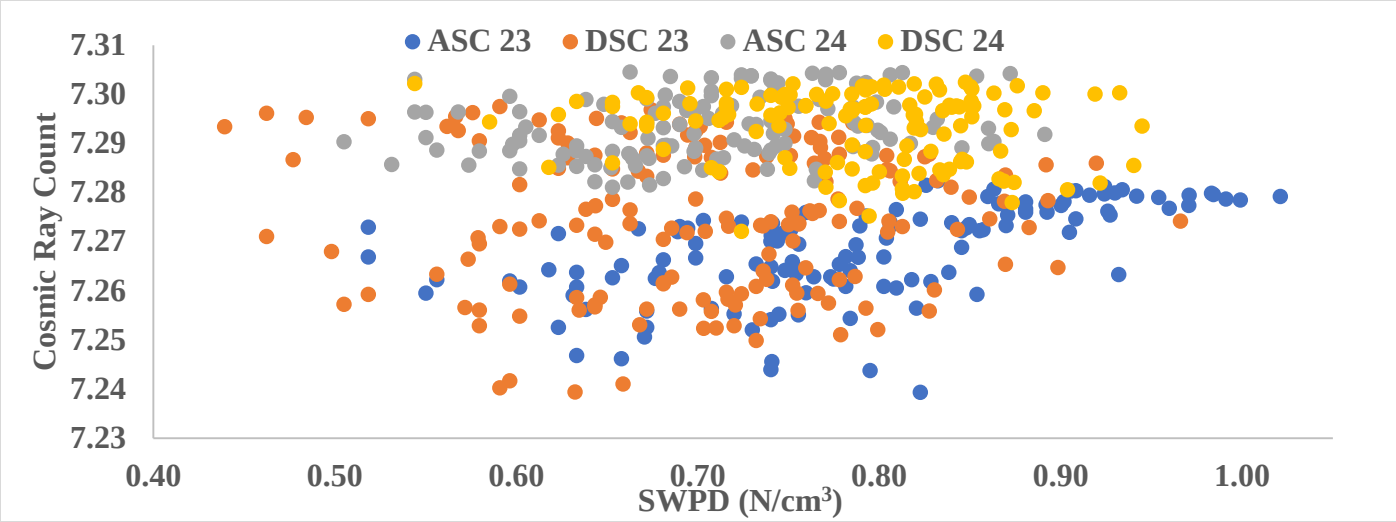

phases show very little sensitivity, with SC 24's DSC phase even showing a slight negative correlation. Overall, the ASC phases are more sensitive to changes in SWPD than the DSC phases in both solar cycles.

Fig 24: log-log Plot of the Monthly Average Values of the Cosmic Ray Intensity vs SWPD for the ASC and the DSC Phases of SC 23 and 24

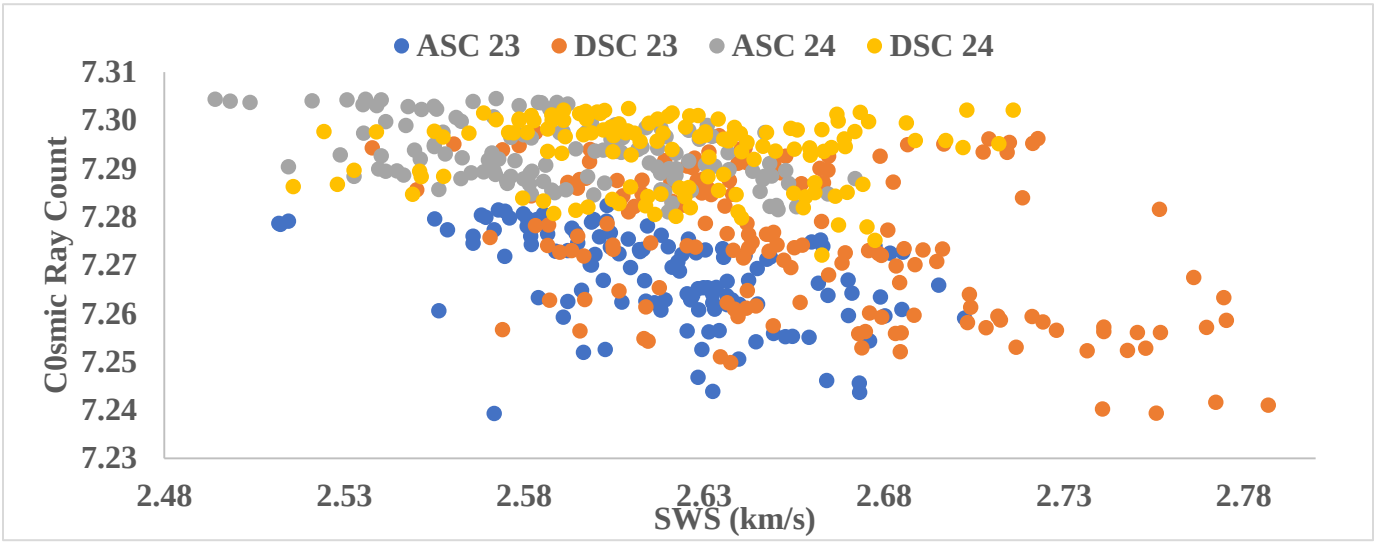

Fig 25: log-log Plot of the Monthly Average Values of the Cosmic Ray Intensity vs SWS for the ASC and the DSC Phases of SC 23 and 24

Fig 25 is the log-log Plot of the Monthly Average Values of Cosmic Ray Intensity vs SWS for the ASC and the DSC Phases of SC 23 and 24**.** The relationships between CR intensity and SWS during the ASC and DSC phases of SCs 23 and 24, given by the result of the linear fits, indicate a moderate negative correlation between CR and SWS during the ASC phase of SC 23. As SWS increases, CR decreases moderately. The DSC phase of SC 23 shows a slightly stronger negative

correlation than the ASC phase. The ASC phase of SC 24 displays a weaker negative correlation compared to SC 23. As SWS increases, CR decreases, but less steeply. The DSC phase of SC 24 shows a very weak negative correlation, almost negligible. The intercepts are higher for SC 23 compared to SC 24, indicating higher baseline CR levels in SC 23. In conclusion, SC 23 shows a stronger and more consistent negative relationship between CR and SWS across both phases, whereas SC 24 shows a weaker and phase-dependent relationship.

Fig 26 is the log-log Plot of the Monthly Average Values of Cosmic Ray Intensity vs SWS for the ASC and the DSC Phases of SC 23 and 24. The correlation coefficients and the regression analysis results are shown in Tables 3 and 4. The relationship between CR intensity and the Kp index (a measure of geomagnetic activity) during the ASC and DSC phases of SCs 23 and 24 exhibits significant variations. In the ASC phase of SC 23, a moderate negative correlation between CR and Kp is observed, while during the DSC phase, it shows a stronger negative correlation. The ASC phase of SC 24 displays a weaker negative correlation compared to SC 23. In the DSC phase of SC 24, the negative correlation is similar to the ASC phase. The DSC phase of SC 23 shows the strongest negative correlation, followed by the ASC phase of SC 23. Both phases of SC 24 show similar and weaker negative correlations. Overall, SC 23 shows a stronger and more variable negative relationship between CR and Kp, while SC 24 shows a consistent but weaker negative relationship in both phases.

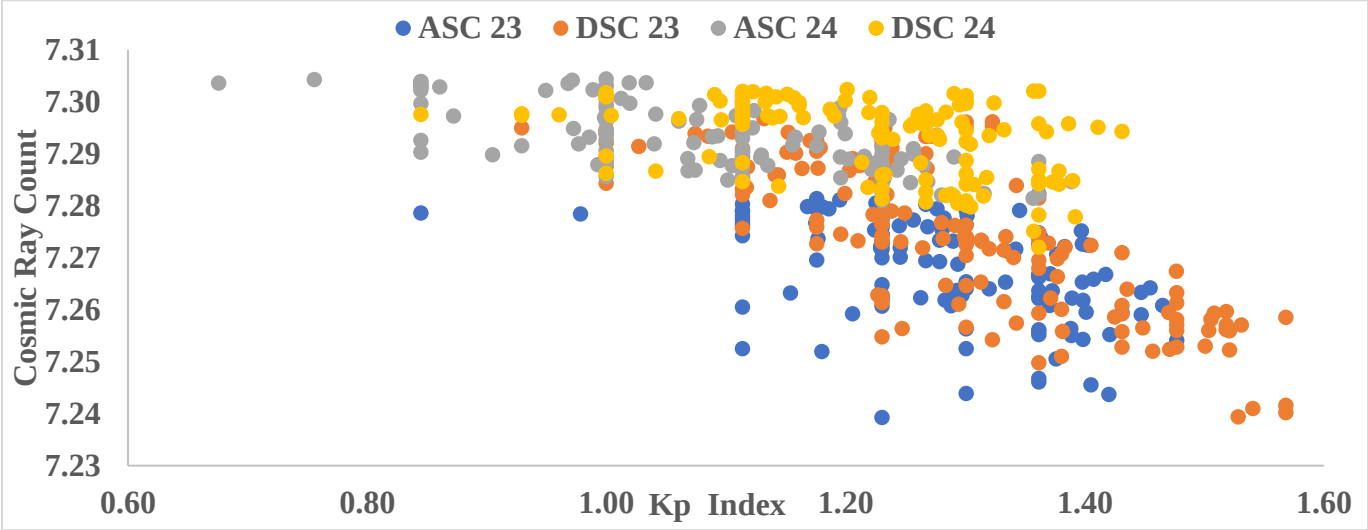

Fig 26: log-log Plot of the Monthly Average Values of the Cosmic Ray Intensity vs Kp for the ASC and the DSC Phases of SC 23 and 24

Fig 27 is the log-log Plot of the Monthly Average Values of Cosmic Ray Intensity vs SWS for the ASC and the DSC Phases of SC 23 and 24. The correlation coefficients and the regression analysis results are shown in Tables 3 and 4. The relationship between CR intensity and the Dst index (which measures geomagnetic activity related to the ring during the ASC and DSC phases of SCs 23 and 24 is given in Table 4 (we have used the absolute value of Dst). During the ASC phase of SC 23, there is a very weak positive correlation between CR and Dst. However, during the DSC phase of SC 23, there is a weak negative correlation. In the ASC phase of SC 24, there is a very weak negative correlation, and in the DSC phase of SC 24, there is a slightly stronger negative correlation compared to the ASC phase of SC 24. In conclusion, the ASC phase of SC

23 shows a very weak positive correlation, while the DSC phase of SC 23 shows a weak negative correlation. The ASC phase of SC 24 shows a very weak negative correlation, and the DSC phase of SC 24 shows a slightly stronger negative correlation.

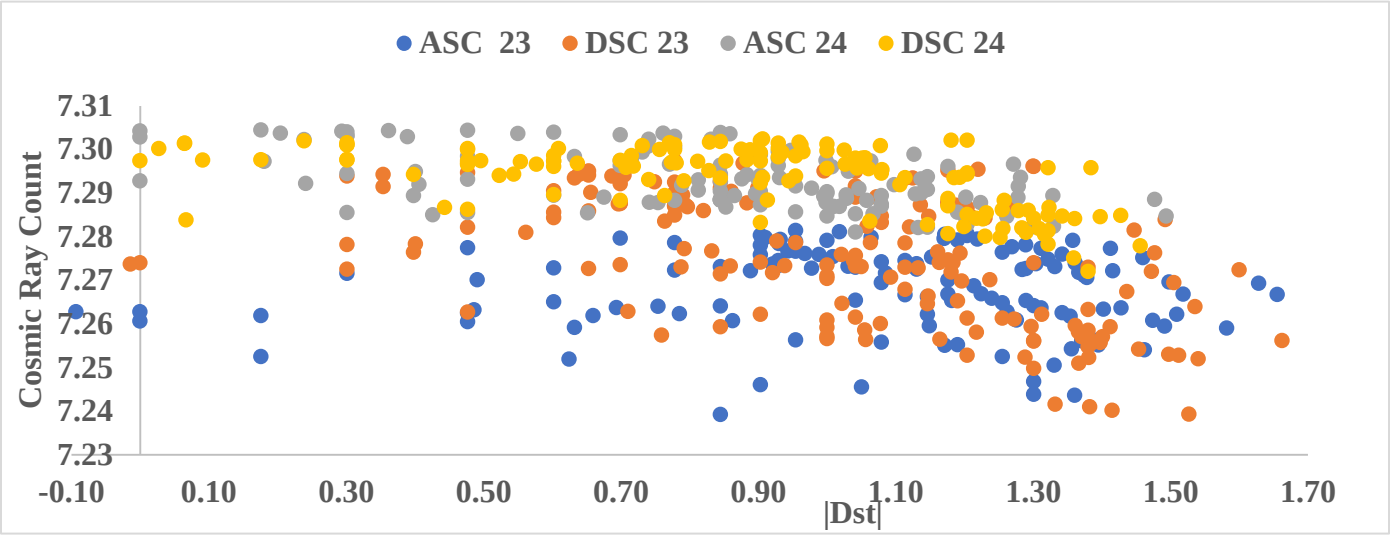

Fig 27: log-log Plot of the Monthly Average Values of the Cosmic Ray Intensity vs |Dst| for the ASC and the DSC Phases of SC 23 and 24

Fig 27 is the log-log Plot of the Monthly Average Values of Cosmic Ray Intensity vs SWS for the ASC and the DSC Phases of SC 23 and 24. The correlation coefficients and the regression analysis results are shown in Tables 3 and 4. The relationship between CR intensity and the ap index (another measure of geomagnetic activity) during the ASC and DSC phases of SCs 23 and 24 shows weak negative correlations with identical slopes. The DSC phase of SC 23 shows a stronger negative correlation, indicating a greater sensitivity to changes in ap during this phase. Overall, SC 23 shows a phase-dependent relationship between CR and ap, with a stronger negative correlation during the DSC phase. SC 24, on the other hand, exhibits a consistent weak negative correlation in both phases. We fitted a multiple linear regression to the CR and SSN, IMF, solar wind parameters, and the geomagnetic indices parameters to observe their impact on CR variations during the ASC and the DSC phases of SC.

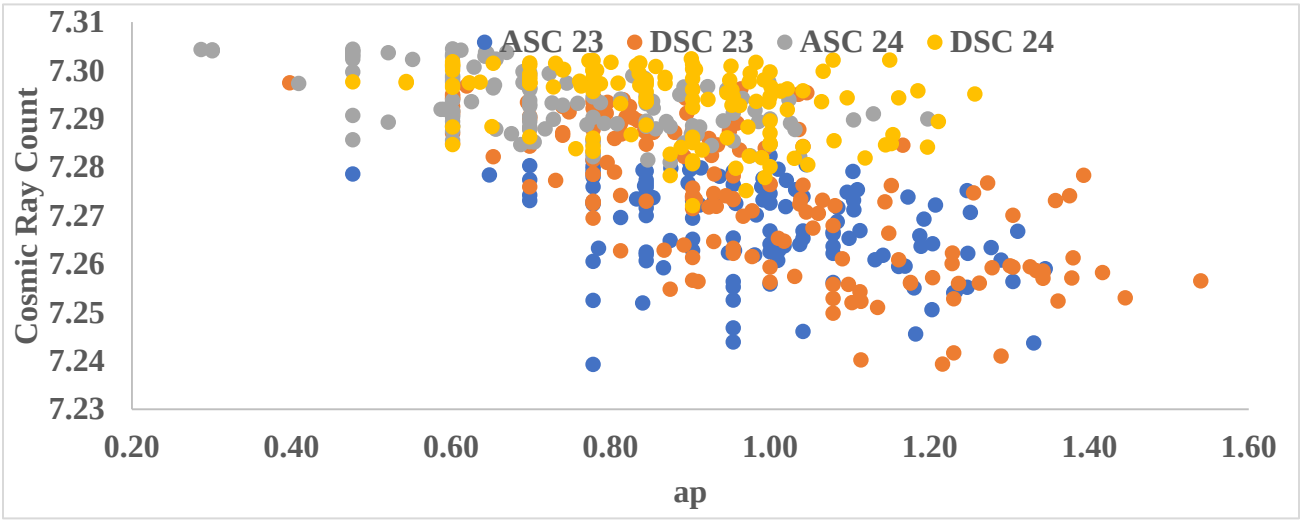

Fig 28: log-log Plot of the Monthly Average Values of the Cosmic Ray Intensity vs ap for the ASC and the DSC Phases of SC 23 and 24

A multiple regression fit to the logarithm values of the studied parameters gives:

$$CR = A + A_1 SSN + A_2 IMF + A_3 SWS + A_4 SWT + A_5 SWPD + A_6 Kp + A_7 |Dst| + A_8 ap \quad 4$$

where A represents the intercept and $A_1 - A_8$ the constant coefficients with the errors associated with each parameter. The values of $A, A_1 - A_8$ for each of the phases is given in Table 5. The intercepts are similar for the phases, an indication that the baseline of CR intensity is nearly similar for SCs 23 &24 (according to Faw and Sculits, 2003) galactic cosmic radiation has been constant in intensity, except for short-term influences of solar activity), but solar modulation is different for each phase and each SC. Hathaway and Rightmire (2010) reported differences in the behavior of the Sun's magnetic field during the ASC phase and the DSC phase, while Upton et al., (2021), reported variations in the meridional flow, which was more pronounced in SC 23 than in the weaker SC 24. These could be the sources of the differences in values and the relationships between the CR, solar wind parameters, and geomagnetic indices during different phases of SC 23 and 24 Hathaway and Rightmire (2010) noted that the transport of magnetic elements across the Sun's surface varies systematically over the SC 23 - faster at minimum and slower at maximum account for the behavior of the distribution at different phases of SC 23, since solar activity is related to CR intensity (e.g. Dorman and Dorman, 1967; Gupta et al., 2005).

Table 5 The Coefficients of Multiple Regression Model Fit to CR Dependence on SSN, IMF, SWS, SWPD, and Geomagnetic Indices for ASC and DSC phases of SC 23 and 24

	ASC 23	DSC 23	ASC 24	DSC 24
Intercept	7.38 ± 0.11	7.30 ± 0.05	7.31 ± 0.05	7.22 ± 0.05
SSN$(\times 10^{-3})$	-6.33 ± 2.64	-4.98 ± 1.54	-5.98 ± 0.93	-2.68 ± 0.98
IMF$(\times 10^{-3})$	-15.81 ± 23.14	-81.42 ± 12.16	-1.46 ± 10.19	-70.71 ± 11.62
SWS$(\times 10^{-3})$	-18.62 ± 53.71	-8.72 ± 25.43	-14.21 ± 26.89	-21.58 ± 28.54
SWT$(\times 10^{-3})$	-8.15 ± 13.21	19.22 ± 10.52	9.81 ± 7.97	16.63 ± 8.85
SWPD$(\times 10^{-3})$	17.57 ± 11.71	16.55 ± 6.97	-4.14 ± 5.24	7.84 ± 6.64
$Kp(\times 10^{-3})$	-10.99 ± 19.24	-35.16 ± 11.65	-14.95 ± 5.04	-22.75 ± 9.15
$\|Dst\|(\times 10^{-3})$	2.97 ± 2.67	5.72 ± 2.25	0.39 ± 1.41	-0.49 ± 1.56
$ap(\times 10^{-3})$	0.92 ± 10.43	-1.38 ± 4.21	-0.21 ± 3.38	8.52 ± 4.48

5 Summary & Conclusion

We have conducted a study on the changes in CR intensities, solar wind parameters, and geomagnetic indices during the ascending and declining phases of SCs 23 and 24, which represent a solar magnetic cycle. Our findings indicate the following:

- Cosmic Ray (CR): CR intensity showed that during the ASC phase of SC 23, there is a higher likelihood of extreme values, unlike the declining phase, which indicates fewer outliers. The CR intensity during the ASC phase of SC 24) shows a slight tendency towards higher values and fewer extreme values. In comparison, the DSC phase of SC 24 has lower values and fewer extreme values but is more evenly spread. These results highlight

differences in the monthly average CR variations between SCs 23 and 24 phases. The average values of CR intensity were higher during the declining phase than the ascending phase.

- Solar Sunspot Number (SSN): The average values of SSN are higher during ASC phases than DSC phases, but DSC phases last longer than ASC phases.
- Interplanetary Magnetic Field (IMF): The distribution is nearly similar for the ASC phases of SCs 23 and 24, and the same applies to the DSC phases, but the ASC phases are different from the DSC phases. The average value of IMF was higher during the ascending phase in SC 23, but in SC 24, the declining phase value was higher.
- Solar Wind Speed (SWS): The ascending phases were similar for both solar cycles, and the declining phases have nearly similar distributions in both cycles.
- Solar Wind Proton Density (SWPD): The distribution showed moderate right skewness during the ascending phases, but the declining phases exhibit different distribution shapes, with SC 23 being leptokurtic and SC 24 being closer to mesokurtic. The average value during SC 23 was higher during the ascending phase, but in SC 24, it was higher during the declining phase.
- Geomagnetic Parameters: The ASC phase of SC 24 shows a greater tendency towards higher values and more frequent extreme events compared to SC 23. The DSC phase of SC 23 exhibits more pronounced right skewness and higher kurtosis, indicating more extreme values.
- The correlation between CR values and the values of other parameters (SSN, IMF, SWS, SWPD, and geomagnetic indices) is similar, but the strength of the relationship differs in each phase.

The differences in solar modulation of cosmic ray flux during the ASC and DSC phases of SCs are traced to several factors including solar magnetic field strength and configuration, heliospheric current sheet tilt angle, CMEs and solar flares, and solar wind speed and density. Potgieter, (2013), observed that during the ASC phase of ASC, the Sun's magnetic field becomes increasingly complex and disorganized due to the rise in solar activity. This increased complexity, along with the intensification of the solar wind, contributes to a stronger modulation of CRs, reducing their flux. During the DSC phases, solar activity wanes, and the magnetic field tends to revert to a simpler, more dipolar configuration, resulting in a weaker modulation effect, allowing more CRs to reach Earth. Heber et al., (2006), noted that the tilt angle of the heliospheric current sheet, which is the wavy surface that separates regions of the Sun's magnetic field with opposite polarities, increases during the solar maximum and the ASC phase of a cycle. This increased tilt makes it harder for CRs to penetrate the heliosphere, reducing their flux. In the DSC phase, the heliospheric current sheet tilt angle decreases, reducing its ability to deflect CRs, which leads to an increase in their flux.

Wiedenbeck et al., (2005), showed that during the ASC phase, the frequency of CMEs and solar flares is higher. These phenomena generate shock waves in the solar wind that can further scatter and block CRs, leading to a reduction in CR flux. In the DSC phase, the frequency of these events decreases, allowing more CRs to reach the inner solar system. According to Badruddin et al., (2007), the speed and density of the solar wind vary across the SC, with higher speeds and densities during the ASC phase. This increased solar wind pressure during solar maxima further shields the solar system from galactic cosmic rays. In contrast, during the DSC phase, the solar

wind becomes less intense, allowing more cosmic rays to penetrate the heliosphere. This contrasted with our results since the median SWS values were higher during the DSC phases than ASC phases for SC 23 and 24, while the median value of SWPD was higher in ASC 23, lower in DSC 23, but higher in DSC 24 than ASC 24 (see Table 1). This implies the complexity of the phases of SC. These factors work in concert to modulate cosmic ray flux differently during the ASC and DSC phases of SCs, reflecting changes in solar activity and the structure of the heliosphere. In conclusion. we analysed the CR intensity variations during the ASC and the DSC phases of SC 23 and 24, our result indicates that CR intensities are modulated in varying degrees during different phases of the solar cycle, and also the modulation is distinct from one solar circle to another.

Furthermore, Koldobskiy et al., (2022) analyzed the time lags between SSN, the open solar flux, representing the heliospheric magnetic variability, and the galactic cosmic ray. They found that GCR variability is delayed concerning the inverted SSN by about eight 27-day Bartels rotations on average, but the delay varies greatly with the 22-year cycle and this could add to the complexity of in the relationships between CR intensities and SSN.

Oloketuyi et al., (2020), found that hat CR intensities undergo an approximate 11-year SC within the heliosphere, which is greatly influenced mainly by solar activities. The cycle formed has its peak at the solar minimum and vice-versa. Our study which is similar to theirs, confirmed that the average sunspot numbers and CR intensities are negatively correlated. The anticorrelations observed from the phase of the cycles are highly significant. Our result also reveals that SWS was found to be anti-correlated with CR intensities in some phases 3 out of the 4 phases studied (though the correlation coefficients obtained indicated mild correlation).

In summary, our analysis of the CR intensity variations during the ASC and the DSC phases of SC 23 and 24 indicates that CR intensities are modulated in varying degrees during different phases of the solar cycle, and also the modulation is distinct from one solar circle to another. If solar flares are assumed to be one of the causes of cosmic radiation, then computer simulations of the sun's magnetic field, such as those by a research group at Harbin Polytechnic University (Jiang et al., 2021), could point the way for our further research.

References

Abe, K., Fuke, H., Haino, S., Hams, T., Hasegawa, M., Horikoshi, A., Itazaki, A., Kim, K. C., Kumazawa, T., Kusumoto, A., Lee, M. H., Makida, Y., Matsuda, S., Matsukawa, Y., Matsumoto, K., Mitchell, J. W., Myers, Z., Nishimura, J., Nozaki, M., Orito, R., et al., (2016). The Astrophysical Journal 822(2), 65-81

Abramowski, A., et al. (HESS Collaboration). (2016) Nature. 531 (7595): 476-479 doi:10.1038/nature17147.

Ackermann, M. Ajello, M., Allafort, A., Baldini, L., Ballet, J., Barbiellini, G., Baring, M. G., Bastieri, D., Bechtol, K., Bellazzini, R., Blandford, R. D., Bloom, E. D., Bonamente, E., Borgland, A. W., Bottacini, E., Brandt, T. J., Bregeon, J., Brigida, M., Bruel, P., Buehler, R., et al., (2013), Science, 339(6121), 807-811, 10.1126/science.1231160.

Adriani,O., Barbarino,G. C., Bazilevskaya,G. A., Bellotti, R., Boezio, M., Bogomolov, E. A., Bonechi, L., Bongi, M., Bonvicini, V., Borisov, S., Bottai, S. Bruno, A., Cafagna, F., Campana, D., Carbone, R., Carlson, P., Casolino, M., Castellini, G., Consiglio, L., De Pascale, M. P. De Santis, C., De Simone, N., Di Felice, V., Galper, A. M., Gillard, L. Grishantseva, W., Jerse, G., Karelin, A. V., Koldashov, S. V., Krutkov, S. Y., Kvashnin, A. N.,Leonov, A., Malakhov, V., Malvezzi, V., Marcelli, L., Mayorov, A. G.,

Menn, W., Mikhailov, V. V., Mocchiutti, E., Monaco, A., Mori, N., Nikonov, N., Osteria, G., Palma, F., Papini, P., ,et al., (PAMELA), (2011), Science 332(6025), 69-72, DOI: 10.1126/science.1199172

Agrawal S.P., Shrivastava, P.K. and Shukla R.P., (1993), Proc. 23rd Int. Cosmic Ray Conf. 3:590,

Aguilar, M., et al., (AMS), (2015a), Phys. Rev. Lett. 114, 171103.

Aguilar, M., et al., (AMS), (2015b), Phys. Rev. Lett. 115, 21, 211101.

Aharonian, F., et al., (H.E.S.S.), (2007). Phys. Rev. D75, 042004

Ahluwalia, H. S., & Ygbuhay, R. C. (2014). Journal of Atmospheric and Solar-Terrestrial Physics, 113, 23-27

Anchordoqui, L., Paul, T., Reucroft, S., Swain, J. (2003), International Journal of Modern Physics A. 18 (13): 222 2366. doi:10.1142/S0217751X03013879.

Archer, A. et al., (VERITAS), (2018), Phys. Rev. D98, 2, 022009.

Aslam, O. P. M., & Badruddin (2012). Solar Physics, 279(1), 269-286.

Aslam, O. P. M., & Badruddin (2015). Journal of Geophysical Research: Space Physics, 120(2), 1081-1094

Auger, P., Ehrenfest, P., Maze, R., Daudin, J. and Robley A. F., (1939), Rev. Mod. Phys 11 (3-4): 288-291, doi:10.1103/RevModPhys.11.288.

Ave, M., Boyle, P. J., Gahbauer, F., Hoppner, C., Hörandel, J. R., Ichimura, M., Müller, D., and Romero-Wolf, A., (2008). Astrophysical Journal, 678, 262, **DOI** 10.1086/529424

Badruddin, M., Yadav, R. S., & Yadav, N. R. (2007). Cosmic ray intensity variations during solar cycle phases: A study of long-term changes. Journal of Atmospheric and Solar-Terrestrial Physics, 69(6), 601-611. https://doi.org/10.1016/j.jastp.2006.11.013

Balasubrahmanyan, V. K. (1969).Solar Physics 7, 39-45, https://doi.org/10.1007/BF00148403,

Balogh, A., Hudson, H.S., Petrovay, K., et al. (2014), Space Sci Rev 186, 1–15. doi.org/10.1007/s11214-014-0125-8

Barichello, J.C., (1978), Solar-Terrestrial Relations? M.Sc. Thesis, Univ. Of Calgary, Canada.

Belov, A., Eroshenko, E., Yanke, V., Oleneva, V., Abunin, A., Abunina, M., Papaioannou, A., Mavromichalaki, H. (2018), Solar Physics 293, 68

Bhattacharya R., Roy M., IJEST, vol. 6, 24 2014.

Blasi, P.; Epstein, R. I.; Olinto, A. V. (2000). The Astrophysical Journal. 533 (2), L123, L126. doi:10.1086/312626.

Blazquez-García, A., Conde, A., Mori, U., Lozano, J. A., (2021), ACM Computing Surveys 54(3):1-33, DOI: 10.1145/3444690Solanki, 2002

Bothmer, V., & Rust, D. M. (2024). Geomagnetic storms of Solar Cycle 24 and their solar sources. *Earth, Planets and Space*. Retrieved from https://earth-planets-space.springeropen.com Earth Planets Space

Castellina, A., Donato, F., In Oswalt, T.D.; McLean, I.S.; Bond, H.E.; French, L.; Kalas, P., (2012), Barstow, M.; Gilmore, G.F.; Keel, W. (eds.). Planets, Stars, and Stellar Systems (1 ed.). Springer. ISBN 978-90-481-8817-8.

Chaurasiya, D. K., Goyal, S., Shrivastava, K., Gupta, R. S., IJIRSET, Vol 17, issue 7, 2023 e-ISSN2319-8753, DOI:10.15680/IJIRSET.2023.1207125. (2023)

Cliver. E.W. \& Ling, A.G. (2001), Astrophys. J, 551 L189-L192.

Conway A. J., (1998), New Astronomy Reviews., 42(5):343-394.

Cramer, D. (1997) Fundamental Statistics for Social Research. Routledge. ISBN 9780415172042,

Denkmayr K., Cugnon P., (1997), Proceedings of the 5th Solar-Terrestrial Predictions Workshop. In R. Heckman, editor. Japan: Communications Research Laboratory. p. 103.

Dorman, I. V. and Dorman, L. I. (1967). J. Geophys. Res., 72, 1513. Doi. 10.1029/JZ072i005p01513
Dumbovic, M., Vrsnak, B., Calogovic, J., Karlica, M., (2011), Astronomy and Astrophysics 531(A91), 1
Echer, E., Lucas, A.d., Hajra, R. et al. (2023), Braz J Phys 53, 79. doi.org/10.1007/s13538-023-01294-w
Echer, E., Rigozo N. R., Souza M. P., et al. (2004), Annales Geophysicae. 22:2239-2243,
Faw, R. E., and Shultis, J. K., (2003), in Encyclopaedia of Physical Science and Technology (Third Edition) ed R. A. Meyers,
Fisher, R.A. (1915), Biometrika 10(4), 507
Forbush, S.E., (1946), Phys. Rev. 70, 771.
Gieseler, J., Heber, B., & Herbst, K. (2017). Journal of Geophysical Research: Space Physics, 122(10), 10964-10979
Gonzalez, W. D., Echer, E., Tsurutani, B. T., & Gonzalez, A. L. C. (2011). Interplanetary Origin of Intense, Superintense, and Extreme Geomagnetic Storms. Space Science Reviews, 158(1), 69-89. doi.org/10.1007/s11214-010-9715-2).
Gopalswamy, N., Yashiro1, S., Mäkelä1, P., Michalek, G., Shibasaki, K., and Hathaway, D. H. (2012), The American Astronomical Society. The Astrophysical Journal Letters, 750(2) doi: 10.1088/2041-8205/750/2/L42
Gopalswamy, N., et al. (2015). The Astrophysical Journal Letters, 804(1), L23. doi.org/10.1088/2041-8205/804/1/L23).
Gupta, M., Mishra, V. K. and Mishra, (2005), 29th International Cosmic Ray Conference Pune 2, 147-150,
Hanslmeier A., Denkmayr K., Weiss P., (1999), Solar Physics. 184(1):213-218.
Hathaway, D. H. \& Upton, L. (2014), Journal of Geophysical Research: Space Physics, doi.org/10.1002/2013JA019432
Hathaway, D. H. and Rightmire, L. (2010), American Astronomical Society, AAS Meeting No. 216, id.319.02; Bulletin of the American Astronomical Society, Vol. 41, p.909.
Heber, B., Fichtner, H., \& Scherer, K. (2006). Solar and heliospheric modulation of galactic cosmic rays. Space Science Reviews, 125(1-4), 81-93. https://doi.org/10.1007/s11214-006-9048-7
Heber, B., Kopp, A., Gieseler, J., Mewaldt, R. A., Möbius, E., & Rice, J. (2009). Modulation of galactic cosmic ray protons and electrons during the unusual solar minimum of 2006 to 2009. The Astrophysical Journal, 699(2), 1956.
Hjorth, J., Bloom, J. S., (2012), In C. Kouveliotou; R. A. M. J. Wijers; S. E. Woosley (eds.). Gamma-Ray Bursts. Cambridge Astrophysics Series. Vol. 51. Cambridge University Press. pp. 169-190.
Hoyt, D. V., Schatten, K. H., (1998) Solar Physics. 179(1):189-219.
Hoyt, D. V., Schatten, K. H.,. (1979), USA: Oxford University Press;
http://www.cosmicrays.unam.mx/.
http://www.nmdb.eu,
http://www.sidc.be/SILSO/.
Iwok, I.A.: 2011, Amer. J. Sci. Ind. Res. 2, 488. American Journal Of Scientific And Industrial Research 2011, Science Huβ, doi:10.5251/ajsir.2011.2.4.488.490
Jiang, C., Feng, X., Liu, R., Yan, X., Hu, Q., Moore R. L., Duan, A., Cui, J., Zuo, P, Wang, Y., and Wei, F., (2021). A fundamental mechanism of solar eruption initiation. *Nat Astron* **5**, 1126–1138 https://doi.org/10.1038/s41550-021-01414-z

Jolliffe, I. T., & Stephenson, D. B. (2012). Forecast Verification: A Practitioner's Guide in Atmospheric Science. Wiley Publishers
Jothe, M. K., Singh, M., Shrivastava, P. K., (2010), Ind. J. Sci. Res. 1, 55
Kane R. P. (2006), Advances in Space Research. 37:1261-1264.
Kass, R. E., Eden, U. T., & Brown, E. N. (2018). Smoothing and inference for time series data. Journal of Time Series Analysis.
Kilpua, E. K. J., Hietala, H., Koskinen, H. E. J., Fontaine, D., & Turc, L. (2015). Journal of Space Weather and Space Climate, 5, A29. doi.org/10.1051/swsc/2015027).
Koldobskiy SA, Kähkönen R, Hofer B, Krivova NA, Kovaltsov GA, Usoskin IG. Time lag between cosmic-ray and solar variability: Sunspot numbers and open solar magnetic flux. Solar Physics. 2022 Mar;297(3):38.
Kuwabara, T., Munakata, K., Yasue, S., Kato, C., Akahane, S., Fujimoto, K., ... & Bieber, J. W. (2009). Journal of Geophysical Research: Space Physics, 114(A5)
Layden A. C., Fox P. A., Howard J. M., et al., (1991), Solar Physics. 132(1):1-40.
Lingri, D., Mavromichalaki, H., Belov, A., Eroshenko, E., Yanke, V.G., Abunin, A., Abunina, M., (2016), Solar Physics 297, 1
Mann, M. E., et al. (2008). Geophysical Research Letters, 35(16), doi.org/10.1029/2008GL034716
Mavromichalaki, H., Papaioannou, A., Plainaki, C., Sarlanis, C., Souvatzolou, G., Gerontidou, M., Papailiou, M., Eroshenko, E., Belov, A., et al., (2011), Advances in Space Research, 47(12), 2210-2222, doi.10.1016/j.asr.2010.02.019
Mavromichalaki, H., Vassilaki, A., and Marmatsouri, E., (1998) Solar Physics 115, 345,
McComas, D. J., et al. (2013) Weakest Solar Wind of the Space Age and the Current 'Mini' Solar Maximum. The Astrophysical Journal, 779(1), 2. doi.org/10.1088/0004-637X/779/1/2
Mishra, W., Sahani P. S., Khuntia, S., Chakrabarty D., (2024), Distribution and recovery phase of geomagnetic storms during solar cycles 23 and 24, Monthly Notices of the Royal Astronomical Society, 530(3), 3171–3182, doi.org/10.1093/mnras/stae1045
Mishra, M.P., (2005), 29th International Cosmic Ray Conference Pune 2, 159-162,
Mishra, V.K., Mishra, A.P. (2016), Indian J Phys 90, 1333-1339, https://doi.org/10.1007/s12648-016-0895-9,
Moraal, H., & McCracken, K. G. (2012). Space Science Reviews, 176(1-4), 299-319.
Okike, O., Alhassan, J.A., Iyida, E.U., Chukwude, A.E., (2021), Monthly Notices of the Royal Astronomical Society 503, 5675
Okike, O., Nwuzor, O.C., Odo, F.C., Iyida, E.U., Ekpe, J.E., Chukwude, A.E., (2020), MNRAS,
Okike, O., Umahi, A.E., (2019), Solar Physics 294(2)
Oloketuyi J, Liu Y, Amanambu AC, Zhao M. Responses and periodic variations of cosmic ray intensity and solar wind speed to sunspot numbers. Advances in Astronomy. 2020;2020(1):3527570.
Onuchukwu C. C. (2018), Phys Astron Int J., 2(4):300-308
Persai, S. K., Jothe, M. K., Singh, M., K Shrivastava, (2015), International Journal of Science and Research (IJSR) Volume 4 Issue 12,
Potgieter, M. S. (2013). Living Reviews in Solar Physics, 10(1), 3. doi.org/10.12942/lrsp-2013-3
Potgieter, M. S. (2013). Solar modulation of cosmic rays, Living Reviews in Solar Physics, 10(3), 1-53. https://doi.org/10.12942/lrsp-2013-3
Ramesh K. B. (2010), The Astrophysical Journal Letters.;712(1):L77–L80

Rangarajan, G.K., Lyemori, T., (1997), Annales Geophysicae 15, 1271–1290. doi.org/10.1007/s00585-997-1271-z
Rees, M., Sargent, W. (1968), Nature 219, 1005–1009. doi.org/10.1038/2191005a0
Richardson, I. G. (2013). Living Reviews in Solar Physics, 10(1), 3. doi.org/10.12942/lrsp-2013-1).
Rudebusch, G. D., & Williams, J. C. (2009). Journal of Business & Economic Statistics, 27(4), 492-503
Ruzmaikin, A. (2001), Space Science Reviews 95, 43–53. doi.org/10.1023/A:1005290116078
Sharma, S., (2008), Atomic and Nuclear Physics. Pearson Education India. p. 478. ISBN 978-81-317-1924-4..
Simpson, J. A., (1983)Annual Review of Nuclear and Particle Science, vol. 33, 323 382 10.1146/annurev.ns.33.120183.001543
Simpson, J. A., (1990), Proc. Int. Cosmic Ray Conf. 12, 187.
Singh, A., Chaudhari, A., Sharma, G., and Singh, A. K., (2024), Research in Astronomy and Astrophysics, 24(2), doi.10.1088/1674-4527/ad1922
Singh, S., Palb, M., Kumar, P., Ranic, A., Thakur, N., Singhd, K., Mishrae, A. P. (2023), 38th International Cosmic Ray Conference (ICRC2023),
Solanki, S. (2002), Astronomy & Geophysics, 43(5), 9-13, doi.org/10.1046/j.1468-4004.2002.43509.x
Solanki, S. (2003),. The Astron Astrophys Rev 11, 153–286. doi.org/10.1007/s00159-003-0018-4
Sparvoli, R., and Martucci, M., (2022), Applied Sciences 2022, 12(7), 3459; doi.org/10.3390/app12073459
Spiegel E. A. (1994), In Lectures on Solar and Planetary Dynamos. In: Proctor MRE, Gilbert AD, editors. UK: Cambridge University Press, 245.
Tsurutani, B. T., Echer, E., Gonzalez, W. D., & Guarnieri, F. L. (2014).. Journal of Geophysical Research: Space Physics, 119 (5), 3716-3719. doi.org/10.1002/2014JA019805).
Tukey, J. W. (1977). Exploratory Data Analysis. Addison-Wesley Publishing Company Reading, Mass. Menlo Park, Cal., London, Amsterdam, Don Mills, Ontario, Sydney XVI, 688 S.
Upton, L., Hathaway, D. H., Sushant, M., (2021), AGU Fall Meeting 2021, held in New Orleans, LA, 13-17 December 2021, id. SH54A-012021AGUFMSH54A..01U
Usoskin, I. G., Huotari, K. A., Kovaltsov, G. A., and Mursula, K. (2005). Journal of Geophysical Research vol. 110, A108, doi: 10, 1029/005 JA 011250,
Usoskin, I. G., Mursula, K., & Kovaltsov, G. A. (2002).. Advances in Space Research, 29(3), 397-404. doi.org/10.1016/S0273-1177(02)00097-3).
Vaclav, C., (2009), Vol. I. Eolss Publishers. p. 165. ISBN 978-1-84826-104-4.
van Allen, J.A., (2000), Geophys. Res. Lett, 27, 2453-2456.
Vannoni, G.; Aharonian, F. A.; Gabici, S.; Kelner, S. R.; Prosekin, A. (2011), Astronomy \& Astrophysics. 536: A56. doi:10.1051/0004-6361/200913568.
White, O., Kopp, G., Snow, M., et al. (2011),. Solar Physics 274, 159-162. doi.org/10.1007/s11207-010-9680-7
Wiedenbeck, M. E., Cohen, C. M., Cummings, A. C., Leske, R. A., Stone, E. C., & von Rosenvinge, T. T. (2005). Observations of solar energetic particles from large CMEs in solar cycles 23 and 24. Astrophysical Journal Letters, 633(1), L103-L106. https://doi.org/10.1086/497631
Xu T., Wu J, Wu Z., et al., (2008), Chinese Journal of Astronomy and Astrophysics. 8(3)337-342.
Zhan L. S., Zhao H. J., Liang H. F., (2003), New Astronomy, 8, 449-456.
Zhang, J., Temmer, M., Gopalswamy, N., et al. (2021). Prog Earth Planet Sci 8, 56 doi.org/10.1186/s40645-021-00426-7

Zweibel, E. G. (2013), Phys. Plasmas 20 (5), 055501 doi.org/10.1063/1.4807033